Plant Physiology Preview. Published on September 28, 2015, as DOI:10.1104/pp.15.00915

Running head:

Role of PNY-PNF in meristem competence to flower

Names of corresponding authors:

Véronique Pautot,
Institut Jean-Pierre Bourgin, UMR1318 INRA-
Agro Paris Tech,
Bâtiment 2,
INRA Centre de Versailles-Grignon
Route de St Cyr (RD10)
78026 Versailles Cedex FRANCE

Telephone: 33(0)130833058
E-mail: Veronique.Pautot@versailles.inra.fr

Shelley R. Hepworth
Department of Biology
Carleton University
1125 Colonel By Drive
Ottawa, Ontario, Canada
K1S 5B6
Telephone: 001-613-520-2600 Ext. 4214
E-mail: shelley_hepworth@carleton.ca

Research area:

Genes, Development and Evolution

Repression of lateral organ boundary genes by PENNYWISE and POUND-FOOLISH is essential for meristem maintenance and flowering in *Arabidopsis thaliana*[1]

Madiha Khan, Laura Ragni[2], Paul Tabb, Brenda C. Salasini, Steven Chatfield[3], Raju Datla, John Lock, Xiahezi Kuai, Charles Després, Marcel Proveniers, Cao Yongguo, Daoquan Xiang, Halima Morin, Jean-Pierre Rullière, Sylvie Citerne, Shelley R. Hepworth*, and Véronique Pautot*

Department of Biology, Carleton University, Ottawa, Ontario, Canada K1S 5B6 (M.K., P.T., B.C.S., S.C, J.L., S.R.H.); National Research Council Canada, Saskatoon, Saskatchewan, Canada S7N 0W9 (C.Y., D.X, R.D.); Department of Biological Sciences, Brock University, St. Catharines, Ontario, Canada L2S 3A1 (X.K, C.D.); Molecular Plant Physiology, Department of Biology, Faculty of Sciences, Utrecht University, Padualaan 8, 3584 CH Utrecht, The Netherlands (M.P.); Institut Jean-Pierre Bourgin, UMR1318 INRA-AgroParisTech, Bâtiment 2, INRA Centre de Versailles-Grignon, Route de St. Cyr (RD10), 78026 Versailles Cedex, France (L.R., H.M., J.-P.R., S.C., V.P.).

PNY-PNF maintain meristem activity essential for flowering by repressing a BOP1/2-ATH1/KNAT6 boundary module

Footnotes:

[1]This work was supported by a Natural Sciences and Engineering Research Council Discovery Grant (no. 327195 to S.R.H.) and Natural Sciences and Engineering Research Council Accelerator and Discovery Grants (no. 429440 and no. 251163 to C.D) and by the European Union Early Stage Training Site VERT (grant no. MEST-CT-2004-7576 VERT to L.R).

[2]Current address: Center for Plant Molecular Biology - ZMBP Developmental Genetics University of Tübingen Auf der Morgenstelle 32 D - 72076 Tübingen, Germany

[3]Current address: University of Toronto Mississauga, 3359 Mississauga Road, Mississauga, Ontario, Canada L5L 1C6

[*]Corresponding authors:
e-mail: pautot@versailles.inra.fr
e-mail: shelley_hepworth@carleton.ca.

Abstract

In the model plant Arabidopsis (*Arabidopsis thaliana*), endogenous and environmental signals acting on the shoot apical meristem cause acquisition of inflorescence meristem fate. This results in new patterns of aerial development, seen as the transition from making leaves to the production of flowers separated by elongated internodes. Two related *BEL1-like* homeobox genes, *PENNYWISE* (*PNY*) and *POUND-FOOLISH* (*PNF*) fulfill this transition. Loss-of-function of these genes impairs stem cell maintenance, and blocks internode elongation and flowering. We show here that *pny pnf* apices misexpress lateral organ boundary genes *BLADE-ON-PETIOLE1/2* (*BOP1/2*) and *KNOTTED*-like from *ARABIDOPSIS THALIANA6* (*KNAT6*) together with *ARABIDOPSIS THALIANA HOMEOBOX GENE1* (*ATH1*). Inactivation of genes in this module fully rescues *pny pnf* defects. We further show that BOP1 directly activates *ATH1* whereas activation of *KNAT6* is indirect. The *pny pnf* restoration correlates with renewed accumulation of transcripts conferring floral meristem identity including *FD*, *SQUAMOSA PROMOTER-BINDING PROTEIN LIKE* genes, *LEAFY*, and *APETALA1*. To gain insight into how this module blocks flowering, we analyzed the transcriptome of *BOP1* overexpressing plants. Our data suggest a central role for the *miR156-SPL-miR172* module in integrating stress signals conferred in part by promotion of jasmonic acid biosynthesis. These data reveal a potential mechanism by which repression of lateral organ boundary genes by PNY-PNF is essential for flowering.

INTRODUCTION

Plant development relies on the activity of the shoot apical meristem (SAM) as a continuous source of founder cells for production of new leaves, shoots, and internodes throughout the life cycle (reviewed in (Aichinger et al., 2012). A tight balance between the allocation of cells to developing primordia and the perpetuation of pluripotent stem cells in the central zone maintains the SAM at a constant size. In Arabidopsis, the vegetative SAM produces leaves in a spiral phyllotaxy with dormant axillary meristems. In conjunction, internode elongation is repressed resulting in a basal rosette. The transition to flowering is governed by internal and external signals that converge at the SAM to promote acquisition of inflorescence meristem (IM) fate (reviewed in (Amasino and Michaels, 2010; Srikanth and Schmid, 2011; Andrés and Coupland, 2012)). This process known as floral evocation results in new patterns of growth at the shoot apex including production of flowers and an increase in stem elongation, called bolting. Lateral organ boundaries are specialized domains of restricted growth that separate meristem and organ compartments and produce axillary meristems (reviewed in (Aida and Tasaka, 2006; Tian et al., 2014)). Early in the transition to flowering, the IM produces cauline leaves and axillary meristems that develop as secondary inflorescences. After several nodes, the IM ceases production of leaves and axillary meristems develop as flowers.

Floral repressors in the SAM block meristem competence to flowering during vegetative stages of development. Major pathways for promotion of flowering work in two ways, via down-regulation of floral repressors in the meristem and via production of factors that promote IM and floral meristem identity (Bernier, 1988; Yant et al., 2010; Srikanth and Schmid, 2011). The switch to flowering is governed by internal signals including age, sucrose content, and gibberellin (GA) in conjunction with external cues based on photoperiod, vernalization, ambient temperature, and responsiveness to light or stress stimuli (reviewed in (Srikanth and Schmid, 2011; Wang, 2014)). Inputs from these different pathways converge to regulate a number of floral integrator genes including *FLOWERING LOCUS T (FT)* which is a central component of the photoperiod response (Andrés and Coupland, 2012; Srikanth and Schmid, 2011). FT encodes a small phosphatidylethanolamine-binding protein that is synthesized in leaves and travels via phloem to the SAM (reviewed in Andrés and Coupland, 2012; Corbesier et al., 2007; Jaeger and Wigge, 2007; Mathieu et al., 2007) where it interacts with the bZIP transcription factor FD to activate genes conferring inflorescence identity, including *SUPPRESSOR OF OVEREXPRESSION OF CONSTANS1/AGAMOUS-LIKE20 (SOC1/AGL20)*, *AGL24*, and *FRUITFULL* (*FUL*) (Abe et al., 2005; Teper-Bamnolker and

Samach, 2005; Wigge et al., 2005). These factors in turn promote the expression of floral meristem identity genes *LEAFY* (*LFY*), *APETALA1* (*AP1*), and *CAULIFLOWER* (*CAL*) whose products confer floral fate (Bowman et al., 1993). In parallel, age-regulated down-regulation of *microRNA156* (*miR156*) stabilizes *mRNA* encoding SQUAMOSA PROMOTER BINDING PROTEIN-LIKE (SPL3), SPL4, and SPL5 transcription factors, which function with FT-FD to specify flower development by directly activating *AP1, LFY,* and *FUL* expression (Yamaguchi et al., 2009; Jung et al., 2012; Wang, 2014). The plant hormone GA is a positive regulator of flowering whose function is more pronounced under short days (SDs) when other regulatory pathways are inactive. Under SDs, GAs activate the transcription of *SOC1* and *LFY* in the shoot apex. Under long days (LDs), GA is not required for activation of *SOC1* but is important for activation of other transcripts at the shoot apex. Its targets include *SPL* genes, whose activation is also directed by SOC1 and FD (Galvão et al., 2012; Porri et al., 2012). How these various pathways are integrated with stress signals is an area of active study (e.g. Yang et al., 2012; Hou et al. 2013; Heinrich et al., 2013; Diallo et al., 2014; Steif et al., 2014).

Members of the THREE-AMINO-ACID-LOOP-EXTENSION (TALE) class of homeodomain transcription factors constitute major regulators of meristematic activity. This family includes KNOTTED1-like (KNOX) and BEL1-like (BLH or BELL) members, which function as heterodimers (reviewed in (Hamant and Pautot, 2010; Hay and Tsiantis, 2010)). *SHOOT MERISTEMLESS (STM)*, which is the founding member of the *KNOX* family in Arabidopsis, is required for SAM initiation and maintenance (Clark et al., 1996; Endrizzi et al., 1996; Long et al., 1996). Other *TALE* members such as *BREVIPEDICELLUS* (*BP*)/*KNOTTED-LIKE FROM ARABDOPSIS THALIANA1* (*KNAT1*), *KNAT6*, *PENNYWISE* (*PNY*) [also known as *BELLRINGER*, *REPLUMLESS*, *VAAMANA*, or *LARSON*], *POUND-FOOLISH* (*PNF*), and *ARABIDOPSIS THALIANA HOMEOBOX GENE1* (*ATH1*) are expressed in the SAM and contribute redundantly with *STM* in meristem initiation and maintenance (Byrne et al., 2000; Belles-Boix et al., 2006; Rutjens et al., 2009).

PNY contributes to meristem maintenance and flowering with its closest relative, POUND-FOOLISH (PNF) (Smith et al., 2004). During vegetative development, the SAM in *pny pnf* mutants frequently terminates with development resuming from leaf-derived axillary meristems, a phenotype linked to reduced expression of *STM* (Smith et al., 2004; Ung et al., 2011a; Ung et al., 2011b). The *pny pnf* double mutant is also non-flowering. The *pny pnf* meristem changes shape in response to floral inductive signals and inflorescence identity genes *SOC1* and *FUL* are up-regulated but *FT* levels are reduced and floral meristem identity

genes *LFY*, *AP1,* and *CAL* are not expressed (Smith et al., 2004; Kanrar et al., 2008). The basis of this phenotype is only partly understood. Ectopic expression of *LFY* in *pny pnf* mutants partially rescues flowering at axillary meristems whilst ectopic expression of *FT* fails to rescue flowering and partially restores internode elongation at length suggesting that FT requires PNY-PNF to initiate flower development (Kanrar et al., 2008). Additional data show that STM functions in association with PNY-PNF to specify flowers via promotion of *LFY* expression (Kanrar et al., 2006; Kanrar et al., 2008). This has led to the proposal that STM/PNY-PNF function together with flowering-time products FT-FD and AGL24-SOC1 to initiate development of reproductive structures, flowers and internodes (Smith et al., 2011). More recently, PNY-PNF were shown to promote the expression of SPL3, 4, and 5 transcription factors that direct activation of floral-meristem identity genes in parallel with FT-FD (Lal et al., 2011). Compatible with this, miR156 is up-regulated in *pny pnf* apices. Ectopic expression of *SPL4* in *pny pnf* restores accumulation of *LFY* and *AP1* transcripts and partially restores flower formation (Lal et al., 2011). However, none of these mechanisms identified to date fully explain the basis of *pny pnf* meristem defects.

In addition to roles in the SAM, these factors have distinct functions in establishing inflorescence architecture. Significant reorganization of *KNOX-BELL* gene expression occurs at the transition to flowering in correlation with new patterns of aerial development (Lincoln et al., 1994; Byrne et al., 2003; Smith and Hake, 2003; Smith et al., 2004; Proveniers et al., 2007; Gómez-Mena and Sablowski, 2008). PNY and BP maintain proper internode patterning *via* the regulation of cell wall remodeling proteins (Mele et al., 2003; Etchells et al., 2012). Mutations in *bp* cause short internodes and downward-pointing flowers whereas mutations in *pny* cause irregular elongation of internodes leading to clusters of flowers on the primary stem with phenotypes enhanced in the double mutant. Studies in Arabidopsis have identified the joint activities of BLADE-ON-PETIOLE (BOP) BTB-ankyrin co-activators and TALE homeodomain transcription factors as important in maintaining lateral organ boundaries (reviewed in (Hamant and Pautot, 2010; Hay and Tsiantis, 2010; Khan et al., 2014)). BP and PNY restrict expression of lateral organ boundary genes *BOP1/2*, *KNAT2, KNAT6*, and *ATH1* to boundaries at the base of the floral shoot in controlling growth patterns in the inflorescence (Ragni et al., 2008; Khan et al., 2012a; Khan et al., 2012b; Zhao et al., 2015). These studies revealed that BOP1/2 function as positive regulators of *ATH1* and *KNAT6* expression whose interacting products form a module that opposes BP-PNY activity in regulating inflorescence

architecture (Rutjens et al., 2009; Li et al., 2012; Khan et al., 2012a; Khan et al., 2012b; Khan et al., 2014).

Here, we investigated the interaction of BOP1/2 with TALE members in flower formation. Our studies reveal that PNY and PNF repress the lateral organ boundary genes BOP1/2 and transcriptional targets *ATH1* and *KNAT6* to maintain meristem integrity and flowering. Inactivation of genes in this module fully rescues *pny pnf* defects in meristem maintenance, internode elongation, and flowering. To gain insight into how this module blocks flowering, we analyzed the transcriptome of *BOP1* overexpressing plants. Our data indicate a role for stress signaling via promotion of jasmonic acid as a potential mechanism for counteracting flowering including responsiveness to GA acting in part via the *miR156-SPL-miR172* module.

RESULTS

Inactivation of *BOP1/2*, *KNAT6*, or *ATH1* rescues meristem maintenance, internode elongation, and flowering defects in *pny pnf*

Previously, we showed that misexpression of boundary genes *BOP1/2*, *KNAT6*, and *ATH1* in *bp* and *pny* internodes perturbs inflorescence architecture through localized restriction of growth. Inactivation of genes in this module fully rescue *pny* defects in internode elongation and phyllotaxy but inactivation of *KNAT2* has no such effect (Ragni et al., 2008; Khan et al., 2012a; Khan et al., 2012b). We anticipated that antagonistic functions of these same genes might cause *pny pnf* defects. The *pnf* single mutant has no obvious phenotype. The *pny* mutant has a functional SAM but apical dominance is reduced, flowering is delayed, and organs are clustered on the primary stem due to irregular internode elongation. In *pny pnf/+* hemizygous plants, these defects are enhanced and stem-pedicel fusions occur (Smith and Hake, 2003; Supplemental Fig. S1A-G). In *pny pnf* double mutants, the SAM terminates after the initiation of 3-5 leaves in a majority of seedlings (Smith et al., 2004; Rutjens et al., 2009). Lateral meristems in the axil of rosette leaves support the continued production of leaves, but flowering and internode elongation are blocked (Smith et al., 2004; Rutjens et al., 2009; Lal et al., 2011). To determine if *BOP1/2*, *KNAT/6* and *ATH1* are required in generating *pny pnf* defects, we constructed *bop1 bop2 pny pnf*, *ath1 pny pnf*, *knat2 pny pnf*, *knat6 pny pnf*, and *knat6 knat2 pny pnf* mutants. We first tested for rescue of *pny pnf* defects in SAM maintenance. Previous studies using the *ath1-1* allele indicated that SAM arrest in triple

mutants with *pny pnf* is markedly enhanced, likely due to the depletion of BELL-STM functional complexes (Rutjens et al., 2009). Here, we repeated the analysis with *ath1-3*, which unlike *ath1-1* and *ath1-4* alleles, produces no full or partial mutant transcript (Supplemental Fig. S2). Whilst 57.7% of *pny pnf* plants showed a meristem arrest, no such arrest was observed in *ath1-3 pny pnf* mutants (Fig. 1 and Material and Methods). Meristem function was also rescued by *bop1 bop2* and *knat6* mutations but not by inactivation of *KNAT2* (Fig. 1). These data suggest that PNY-PNF/STM antagonize the activity of lateral organ boundary genes to maintain stem-cell identity. Flower formation, internode elongation, and organ fusion defects were also rescued in *bop1 bop2 pny pnf*, and *knat6 pny pnf* or *ath1-3 pny pnf* triple mutants in comparison to *pny pnf* and/or *pny pnf*/+ plants (Fig. 2A-H; Supplemental Fig. S3). Quantitative phenotypic analyses showed that inflorescence architecture of *bop1 bop2 pny pnf, ath1 pny pnf,* and *knat6 pny pnf* mutants was similar to wild type plants (Supplemental Fig. S4). In contrast, *knat2 pny pnf* mutants remained non-flowering (Fig. 2I).

Overexpression studies further support a role for *BOP1/2*, *ATH1*, and *KNAT6* in the same genetic pathway. Plants that overexpress *BOP1/2* are late flowering with shortened internodes and clustered fruits similar to *pny* and *pny pnf*/+ mutants (Supplemental Fig. 1A-C; (Norberg et al., 2005; Ha et al., 2007; Khan et al., 2012b). Plants overexpressing *ATH1* and occasionally *KNAT6* have similar defects that mimic the inflorescence architecture of *pny* and *pny pnf*/+ mutants (Supplemental Fig. S1B-I; Proveniers et al., 2007; Gómez-Mena and Sablowski, 2008; Shi et al., 2011). The most severe *KNAT6* transgenic lines were strongly inhibited in their development and failed to flower (Supplemental Fig. S1JK). Collectively, these data indicate that PNY-PNF play no essential function in meristem/boundary maintenance, internode elongation, and flowering beyond repression of BOP1/2 and ATH1/KNAT6.

***BOP1/2*, *ATH1*, and *KNAT2/6* expression domains are expanded in *pny pnf* apices**

Inflorescence defects in *pny* mutants correlate with an expanded pattern of expression for *BOP1/2*, *ATH1*, and *KNAT2/6* in internodes (Ragni et al., 2008; Khan et al., 2012a; Khan et al., 2012b). We therefore examined the expression patterns of these genes in *pny pnf* apices. In wild-type apices, *BOP2* transcripts accumulate in the adaxial domain of floral meristems until late stage 2 when expression shifts to the boundary with the cryptic bract. Expression is found in the boundary domains of older flowers (Fig. 3A; see also (Xu et al., 2010). *ATH1* transcripts are expressed in incipient floral primordia and in the dome of stage 2 floral

primordia in a pattern similar to *KNAT2*. *KNAT6* transcripts are localized to boundary domains flanking the IM and in flowers also overlapping with *KNAT2* (Fig. 3B-D). In *pny pnf* apices, the domain of expression for all of these genes expands into the central and rib zones of the meristem (Fig. 3E-H). This was also observed for *BOP1* using a *BOP1-GUS* line (Supplemental Fig. S5). Misexpression of these genes likely begins during the vegetative stage based on analysis of *BOP2:GUS* lines (data not shown) consistent with SAM structural defects (Ung et al., 2011). Little or no misexpression was observed in *pny* or *pnf* control apices (Supplemental Fig. S6). These data confirm that *pny pnf* defects are due to misexpression of *BOP1/2*, *ATH1*, and *KNAT6* in the meristem. We next examined regulatory interactions between these genes in the pathway.

ATH1 is a direct target of BOP1

BOP1/2 were previously shown to promote the expression of *ATH1* and *KNAT6* and require these activities to exert changes in inflorescence (Khan et al., 2012a; Khan et al., 2012b). To test if *ATH1* and/or *KNAT6* are immediate transcriptional targets of BOP1/2, we used a transgenic line expressing a translational fusion of BOP1 to the steroid-binding domain of the rat glucocorticoid receptor (Lloyd et al., 1994). This dexamethasone (DEX) inducible system was used previously to show that BOP1 directly activates the transcription of *ASYMMETRIC LEAVES2* in leaves (Jun et al., 2010). Function of the BOP1-GR fusion protein was confirmed by expressing it under the control of a *BOP1* native promoter and observing efficient complementation of *bop1 bop2* leaf and abscission defects upon addition of DEX (Supplemental Fig. S7). Direct regulation of *ATH1* and/or *KNAT6* was tested using the BOP1-GR fusion protein expressed in wild-type plants under the control of a double 35S promoter. *D35S:BOP1-GR* plants treated with DEX for four weeks had shortened internodes and clustered fruits similar to *bop1-6D* mutants, which constitutively overexpress *BOP1* (Fig. 4A-D; Norberg et al., 2005). Transcripts for *ATH1* were increased 13.29-fold and transcripts for *KNAT6* were increased 2.59-fold in *bop1-6D* internodes compared to wild-type (Fig. 4E). Similarly, *D35:BOP1-GR* plants treated with DEX for four weeks showed a 6-fold upregulation of *ATH1* transcript (Fig. 4E). After 2 and 4 hours of DEX treatment, transcript levels for *ATH1* were at least 2-fold higher but *KNAT6* transcript levels showed no increase relative to Mock-treated control plants (Fig. 4F; 24 hr timepoint not shown). Rapid activation of *ATH1* suggested that its induction by BOP1 may be direct. We tested this by analyzing *ATH1* and *KNAT6* expression in response to DEX induction in the presence of the protein synthesis inhibitor cycloheximide (CHX). After 2 and 4 hours of combined treatment with

DEX and CHX, *ATH1* transcripts were increased 5-fold to 7.5-fold relative to CHX-treated control plants. *KNAT6* transcripts were increased up to 2-fold after combined DEX+CHX treatment but not after DEX alone. Presumably, this is an indirect effect of BOP1 dependent on repression of protein synthesis. These data are consistent with *ATH1* being a direct target of BOP1 and *KNAT6* being an indirect target.

To examine tissue specifity of this interaction, expression of 3.3-kb and 2-kb *ATH1p:GUS* reporter genes expressed in *D35S:BOP1-GR* (see Materials and Methods) were monitored for induction by DEX. Consistent with previous reports (Proveniers et al., 2007; Gómez-Mena and Sablowski, 2008) these reporters were expressed in shoot apices, leaves, floral organ abscission zones, and weakly in the stem. After 4 hours of DEX treatment, GUS activity was enhanced relative to Mock-treated controls for both promoter lines in all tissues (Fig. 5A-H). These data confirm that the *ATH1* promoter is responsive to BOP1 induction.

BTB-ankyrin proteins including BOP1/2 have no DNA-binding domain and interact with TGA bZIP binding factors for recruitment to DNA (Després et al., 2000; Hepworth et al., 2005; Xu et al., 2010; Khan et al., 2014). Direct association of BOP1 with the *ATH1* promoter was tested by chromatin immunoprecipitation (ChIP) using an anti-GR antibody followed by qRT-PCR. Leaf material was collected from *BOP1p:BOP1-GR bop1 bop2* flowering plants. Assays were performed using 8 sets of primers spanning 2178 base pairs of genomic sequence upstream of the *ATH1* transcription start site based on regions enriched in TGA bZIP binding sites (Fig. 5I and Supplementary Table S3). Motifs that match or closely match consensus binding sites for TGA factors are also found in the intragenic and 3'-UTR of the *ATH1* genomic sequence (data not shown). Quantitative analysis by qRT-PCR revealed at least one position in the *ATH1* promoter (Site IV) showing a reproducible 1.77-fold enrichment of BOP1 protein in DEX-treated plants (Fig. 5J). ChIP assays performed using the Mock control showed no significant enrichment at this position nor at the control *UBQ5* genomic region. Site IV (nt –2686 to -2577) is located approximately 1515 base pairs upstream of the *ATH1* transcription start site and found within the 3.3-kb *ATH1p:GUS* construct that is responsive to BOP1 induction in leaves and inflorescences (Fig. 5). Site VII (nt –1529 to -1416) was identified as a second potential binding site. Taken together, these data support that BOP1 directly associates with the *ATH1* promoter *in vivo* to regulate its transcription.

Restored accumulation of flowering transcripts in *pny pnf* apices following rescue by inactivation of *BOP1/2*, *KNAT6*, and *ATH1*

Non-flowering *pny pnf* apices accumulate *SOC1* and *FUL* transcripts markers of inflorescence identity but fail to accumulate *FT* or *LFY*, *AP1* and *CAL* markers of floral fate (Smith et al., 2004; Kanrar et al., 2008). Accumulation of *SPL3*, *SPL4,* and *SPL5* transcripts are also diminished in *pny pnf* apices (Lal et al., 2011). Flowering time of wild-type plants was compared to *bop1 bop2 pny pnf*, *knat6 pny pnf*, and *ath1 pny pnf* mutants to further quantify rescue. Fig. 6A shows that flowering time for *knat6 pny pnf* mutants and wild-type control plants was similar. Flowering time of *bop1 bop1 pny pnf* mutants was slightly delayed (+3.6 days) and flowering time of *ath1 pny pnf* mutants was slightly earlier (-6.9 days) than wild-type consistent with parental controls (Fig. 6A; see also Xu et al., 2010). To test if inactivation of *BOP1/2*, *ATH1*, and *KNAT6* correlates with restored expression of meristem identity genes in *pny pnf* apices, we measured relative transcript abundance in wild-type and mutants. Twenty-five-day-old plants grown under SDs were transferred to LDs to induce flowering. Apices were harvested 12 days later. The floral transition was complete for all genotypes at this timepoint. Fig. 6B confirms that *SOC1* and *FUL* transcripts are relatively unchanged in wild-type compared to mutants. Fig. 6B also shows that low to undetectable levels of *FD*, *LFY*, *AP1*, and *CAL* transcript in *pny pnf* apices resumed expression in triple and quadruple mutants except for *CAL* which remained low in *bop1 bop2 pny pnf* apices. Transcripts for *FUL*, *LFY*, *AP1,* and *CAL* were elevated in *ath1 pny pnf* apices consistent with earlier flowering. Fig. 6C shows that patterns of *miR156* and *SPL* transcript accumulation in triple and quadruple mutants are likewise restored to resemble wild-type. Collectively, these data show that PNY-PNF are dispensible for flowering when BOP1/2, ATH1, and KNAT6 activities are eliminated.

BOP1 **overexpression mimics** ***pny pnf*** **defects in** ***SPL*** **transcript accumulation and responsiveness to GA**

Given that *pny pnf* mutants misexpress *BOP1/2*, we used transcript profiling to test if dwarfism and late flowering exhibited by the gain-of-function *bop1-6D* mutant impacts similar pathways. We first monitored the accumulation of *miR156* and *SPL* transcripts in *bop1-6D* internodes for comparison to *pny pnf* using qRT-PCR (Fig. 7A). These data show that *miR156* transcripts in *bop1-6D* are 1.4-fold upregulated relative to wild-type. In addition, *SPL* transcripts in *bop1-6D* were significantly down-regulated with the exception of *SPL5*. These data suggest that *bop1-6D* partially mimics *pny pnf* (compare Fig. 6C and Fig. 7A).

To further explore similarities and differences between these two mutants, we examined transcripts involved in the regulation of GA which is a positive regulator of internode elongation and flowering (Mutasa-Göttgens and Hedden, 2009; Porri et al., 2012). The expression levels of genes required for GA biosynthesis, catabolism, and DELLA repressors of GA signaling were monitored by qRT-PCR in *pny pnf* apices and in *bop1-6D* apices and internodes and revealed similar patterns (Fig. 7BCD). In both genotypes, there was little or no change in *KS* transcript but *GA20ox1* transcripts were significantly increased (Fig. 7CD; (Yamaguchi, 2008). In *bop1-6D*, there was a compensatory decrease in *GA3ox1* transcripts functioning later in the biosynthetic pathway (Fig. 7D; Yamaguchi, 2008). In internodes, there was also a compensatory increase in *GA2ox7* transcripts required in catabolism (Fig. 7BD; Yamaguchi, 2008). All five *DELLA*s encoding repressors of GA signaling were upregulated in *pny pnf* whereas selective upregulation of *RGL3* was observed in *bop1-6D* (Fig. 7CD). These data indicate that GA homeostasis is disrupted in both mutants. Nevertheless, deficiency alone does not account for phenotypic defects. Spray treatments with GA_3 failed to rescue flowering in *pny pny* nor enhance internode elongation in *bop1-6D*, although this mutant flowered 4 days earlier than Mock-treated control plants (Fig. 7EF; see also Smith et al., 2004)). In conclusion, *SPL* transcript accumulation and responsiveness to GA are blocked in both mutants. We therefore used microarray analysis of *bop1-6D* internodes to identify additional factors that might antagonize flowering and internode elongation in these mutants.

Overexpression of *BOP1* activates stress pathways and promotes accumulation of jasmonic acid as a mechanism for repression of growth and flowering

The transcriptomes of *bop1-6D* versus wild-type internodes were assessed by microarray (see Materials and Methods). Gene Ontology (GO) analysis of differentially regulated genes revealed significant enrichment of terms associated with response to biotic and abiotic stress stimuli (Supplemental Table S1). Response to jasmonic acid (JA) stimulus (GO:009753) was at the top of the list, but other hormone pathways associated with stress showed similar enrichment. In descending order these were response to salicylic acid stimulus (GO:0009751), response to ethylene stimulus (GO:009723) and response to abscisic acid stimulus (GO:0099737). These data suggest that *bop1-6D* plants have heighted expression of stress-related genes. Trade-offs between plant defense and plant growth are well-established in the recent literature (Navarro et al., 2008; Wild et al., 2012; Yang et al., 2012; Wild and Achard, 2013) so we further explored this mechanism. First, we specifically examined floral repressors in the microarray using a candidate gene approach (Fig. 8A). This analysis

382 revealed up-regulation of DELLA, FLOWERING LOCUS C (FLC-like) and APETALA2-
383 like (AP2-like) members. However, the highest-fold changes were observed among
384 AP2/ERF-like factors that repress growth and flowering under stress conditions (Magome et
385 al., 2004; Magome et al., 2008; Kang et al., 2011; reviewed in Licausi et al., 2013). To
386 validate these findings, selected transcripts were quantified by qRT-PCR using independently
387 isolated tissue samples. Floral repressor transcript profiles of *bop1-6D* and *pny pnf* apices
388 genotypes showed strong agreement (Fig. 8B). Consistent with the microarray, no significant
389 change was observed for *FLC*, but transcripts encoding AP2-like repressors *TARGET OF*
390 *EAT2* (*TOE2)* (1.6 to 4-fold) and *SCHLAFMUTZE* (*SMZ)* (8.5 to 21-fold) were highly
391 upregulated compared to wild-type. The highest fold changes (6.2 to 454-fold) were observed
392 for stress-induced AP2/ERF floral repressor trancripts including *DWARF AND DELAYED*
393 *FLOWERING1* and *2* (*DDF1/2*) whose products inhibit growth by reducing bioactive
394 gibberellin content (Magome et al., 2004; Magome et al., 2008; Kang et al., 2011; reviewed in
395 Licausi et al., 2013).

396 Inspection of the microarray also showed an increase in expression of biosynthetic enzymes
397 for JA (Fig. 9AB). Validation of these data by qRT-PCR confirmed significant upregulation
398 of transcripts involved in JA biosynthesis in *bop1-6D* and *pny pnf* tissues (Fig. 9C). To
399 determine if these increases reflect changes in hormone accumulation in plants, JA levels
400 were quantified in internodes and buds from *bop1-6D* and *pny pnf* apices (Material and
401 Methods). BOP1 overexpressing plants showed 2.5-fold higher levels of JA relative to wild-
402 type plants (Fig. 9D). Conversely, hormone levels were decreased in *bop1 bop2* compared to
403 wild-type control plants. *Pny pnf* apices showed 1.5-fold higher levels of JA relative to wild-
404 type control apices at the same stage of development (Fig. 9D). These data suggest that
405 BOP1/2 promote JA production.

406 To further examine JA effects on reproductive plant development, methyl jasmonate (MeJA)
407 was applied to wild-type and *pny* plants grown under LDs (Fig. 10). Plants of both genotypes
408 treated with MeJA developed a compact rosette with small dark green leaves, similar to *bop1-*
409 *6D* mutants (Fig. 10A-C). Wild-type plants treated with MeJA showed partial loss of apical
410 dominance similar to *pny* mutants (Fig. 10D-G). Plants in both treatment populations were
411 late flowering with short internodes relative to Mock-treated control plants (Fig. 10D-G) and
412 similar to *pny pnf*/+ mutants (Supplemental Fig. S1A-G). Organ fusions or clusters were not
413 observed. In both wild-type and *pny* populations, a small subset of plants developed a
414 disordered rosette phenotype similar to *pny pnf* mutants and were non-flowering after 10

weeks (data not shown). No such defects were observed in Mock-treated control plants. Thus, treatment of wild-type plants with exogenous MeJA mimics the phenotype of *bop1-6D* and *pny* or *pny pnf*/+ plants.

In parallel, we tested if reducing JA content rescues internode elongation or flowering in *pny pnf* and/or *bop1-6D* mutants by crossing them to the *aos* mutant which is defective in allene oxide synthase and JA synthesis (Park et al., 2002; Fig. 7B and Fig. 10). Triple mutants with *pny pnf* remained non-flowering even with addition of exogenous GA_3 (Fig. 10H and data not shown). However, quantitative analysis of *bop1-6D aos* double mutants revealed a small but significant ($p \leq 0.0001$) increase in flowering-time (+1.8 days) and plant height (+1.5 cm) compared to *bop1-6D* siblings in a segregating population (Fig. 10IJ). These data provide evidence that modulation of growth by jasmonic acid is a potential factor in conditioning *bop1-6D* and *pny pnf* phenotypic defects.

DISCUSSION

Floral evocation is dependent on SAM restructuring to form an IM (Bernier, 1988). The TALE homeodomain PNY and PNF transcription factors are essential for this process by permitting responsiveness to floral inductive signals (Smith et al., 2004; Kanrar et al., 2008; Lal et al., 2011; Smith et al., 2011; Ung et al., 2011a; Ung and Smith, 2011b). In *pny pnf* mutants, meristems support the production of leaves but internode elongation and flower initiation are blocked.

In this article, we characterized the interaction of PNY and PNF with lateral organ boundary factors BOP1/2 and a pair of downstream effectors: the KNOX-BELL homeodomain factors KNAT6 and ATH1. We show that misexpression of these genes in *pny pnf* apices blocks floral evocation (Fig. 11). Inactivation of *BOP1/2* and *ATH1* or *KNAT6* fully restores *pny pnf* defects in meristem and boundary maintenance, stem elongation and restores expression of floral-meristem identity genes to allow flowering. Remarkably, other factors compensate for the loss of these genes in maintaining the SAM and responsiveness to floral inductive signals. Thus, PNY and PNF allow flowering by excluding boundary genes from the meristem. Similar antagonistic interactions for PNY or BP with members of the BOP1/2-ATH1/KNAT6 module function in various other developmental contexts including abscission, fruit patterning, and inflorescence architecture (Ragni et al., 2008; Shi et al., 2011; Khan et al., 2012; Khan et al., 2012; Li et al., 2012).

We further investigated the organization of this module and its transcriptional targets. Our data show that BOP1 is a direct regulator of *ATH1* whereas promotion of *KNAT6* is probably indirect. Indeed, DEX + CHX treatment of *35S:ATH1-GR* plants produces rapid induction of *KNAT6* transcript and reporter gene expression is missing at boundaries in *ath1-3* but not *bop1 bop2* mutants suggesting a direct requirement for ATH1 (data not shown). BOP1/2 co-activators are recruited to DNA via interactions with TGA bZIP transcription factors (Hepworth et al., 2005, Xu et al., 2010). These TGA factors remain unknown in the context of flowering, but several candidates are being investigated (Fig. 11). Transcript profiling was used to probe how this module blocks flowering. Comparison of the gain-of-function *bop1-6D* mutant and *pny pnf* showed similar transcriptional defects in core pathways controlling flowering. Our data are consistent with the model that BOP1/2-ATH1/KNAT6 boundary genes activate stress pathways that promote JA biosynthesis which directly or indirectly interferes with signals integrated by the *miR156-SPL-miR172* module to antagonize IM function (Fig. 11). Details of this model are discussed below.

The *miR156-SPL-miR172* module as a hub for integration of flowering signals

The *miR156-SPL-miR172* module is a core pathway for integration of flowering signals including age, sugar, gibberellin, and stress (Huijser and Schmid, 2011; Cho et al., 2012; Proveniers et al., 2013; Cui et al., 2014; Stief et al., 2014; Wang, 2014). In brief, *miR156* levels decline with age leading to a concomitant increase in abundance of *SPL* transcripts whose products act on distinct targets in leaves and the shoot apex to promote flowering (Wu and Poethig, 2006; Wang, 2009; Wu et al., 2009). SPL3 and SPL9 members in the SAM directly promote the activation of floral-meristem identity genes (Wu et al., 2009; Yamaguchi et al., 2009). SPL9-like members have additional functions in leaves where they activate the transcription of *miR172b*, which lowers the abundance AP2-like floral repressor transcripts allowing accumulation of *FT* mRNA (Zhu and Helliwell, 2011; Matsoukas et al., 2012; Wang, 2014).

Significant reduction of *miR156*-regulated *SPL* transcripts was observed in *pny pnf* and *bop1-6D* mutants. This reduction is likely driven by multiple factors including lower levels of *FD,* whose product recruits FT to the promoter of *SPLs* for activation (Jung et al., 2012; see also Andrés and Coupland, in this issue) and higher steady state levels of *miR156* (see also Lal et al., 2011). An increase in *miR156* was less marked in *bop1-6D* suggesting that the reduction in *SPL* transcript is mediated *via miR156* and other regulators. These data are consistent with

previous work showing that *SPL3/4/5* transcripts are reduced in *pny pnf* apices and partly account for non-flowering (Lal et al., 2011). Transgenic *pny pnf* plants expressing a *miR156*-resistant form of *SPL4* were restored for *LFY* and *AP1* expression but only partly restored for flowering suggesting that multiple *SPL* factors are involved (Lal et al., 2011).

Concomittantly, trancripts encoding *miR172*-regulated AP2-like repressors of flowering and internode elongation were elevated in *bop1-6D* and *pny pnf* mutants. This group of repressors includes AP2, SMZ, TOE1, TOE2, and TOE3 with overlapping functions (Aukerman and Sakai, 2003; Jung et al., 2007; Mathieu et al., 2009; Yant et al., 2010). SMZ and presumably other members of this family delay flowering through the direct repression of *FT* and promotion of *miR156* (Mathieu et al., 2009; Yant et al., 2010). Of these, *TOE2* and *SMZ* show consistent upregulation in the transcriptome of *bop1-6D* and *pny pnf* apices. Thus, overexpression of AP2-like members in *bop1-6D* may be a route to restricting internode elongation and flowering.

Integration with signals for stress and carbohydrate metabolism

Stress and sugar signals are also integrated through the *miR156-SPL-miR172* module to control flowering (reviewed in Wang, 2014). Recent studies address the mechanism. One study shows that *miR156-SPL3* delays flowering under cool ambient temperatures via regulation of *FT* (Kim et al., 2012). Similarly, plants overexpressing *miR156* are late flowering with increased tolerance to stress linked to downregulation of *SPL9* (Cui et al., 2014). Stief et al. (2014) further showed that heat stress induces *miR156* isoforms linked to downregulation of *SPL9*-like transcripts (*SPL2*, *SPL9*, *SPL11*) and delayed flowering. Induction of *miR156h* in this cascade is predicted to target the pectin methylesterase inhibitor *At5g38610* which may affect bolting (Stief et al., 2014). PNY/BLR control inflorescence patterning by regulating cell wall modification enzymes including pectin methylesterases which loosen cell walls in the stem to promote internode elongation and in the SAM to facilitate organ initiation (Etchells et al., 2012; Peaucelle et al., 2011). *At5g38610* and related genes are upregulated in the transcriptome of *bop1-6D* internodes whereas PNY-regulated *PME5* is downregulated consistent with dwarf stature (data not shown; Peaucelle et al., 2011).

The *miR156-SPL-miR172* module is also a sensor for nutrients. A developmental decline in *miR156* is partially mediated by sugars produced by photosynthesis which accumulate with age (Proveniers, 2013; Yang et al., 2013; Yu et al., 2013). Global transcript changes in *bop1-*

6D mutants are characterized in large part by alterations in stress signaling and carbohydrate metabolism (Supplemental Table S1). GO enrichment analysis of the *bop1-6D* transcriptome identifies significant down-regulation of cellular carbohydrate metabolism, metabolic processes, and nitrogen metabolism, which potentially act to restrict sucrose availability at the shoot apex (Supplemental Table S1). Part of these changes were confirmed in *pny pnf* mutants suggesting that resources are allocated towards defense in detriment to flowering.

Integration with gibberellin pathways

Our study also identifies GA pathway changes in *bop1-6D* and *pny pnf* mutants detrimental to flowering. In wild-type plants, bioactive GA content increases 100-fold at the transition (Eircksson et al., 2006) facilitating internode elongation and flowering by lowering the abundance of DELLA repressors (Mutasa-Göttgens and Hedden, 2009; Galvão et al., 2012; Porri et al., 2012; Yu et al., 2012) GA signals are partly integrated through the *miR156-SPL-miR172* module based on studies showing that GA/DELLA regulate *SPL3/4/6/9* transcription at the shoot apex independent of SOC1 (Galvão et al., 2012; Porri et al., 2012). Physical interaction of RGA DELLA with SPL9 interferes with activation of MADS-box flowering genes at the shoot apex and with activation of *miR172b* in leaves thereby maintaining AP2 and AP2-like repression of stem elongation and flowering (reviewed in Wang, 2014). Other nodes of integration with the *miR156-SPL-miR172* module are likely given that GA treatment does not markedly accelerate flowering in a *miR156* overexpression line (Yu et al., 2012). Transcriptional profiling in *bop1-6D* and *pny pnf* plants indicate complex changes affecting biosynthesis, catabolism, and/or signaling. Exogenous GA fails to restore flowering in *pny pnf* apices nor internode elongation in *bop1-6D*, similar to transgenic plants overexpressing *ATH1* (Smith et al., 2004; Gómez-Mena and Sablowski, 2008; this study) consistent with blockage at multiple steps. Four of five DELLA transcripts are significantly upregulated in *pny pnf* apices whereas *RGL3* is selectively upregulated in *bop1-6D*. Transcript accumulation and steady state level of protein show strong correlation in previous studies (Wild et al., 2012). Transgenic plants overexpressing DELLAs or DELLA proteins resistant to degradation are dwarf and late-flowering similar to *bop1-6D* plants (Dill et al., 2004; Hamama et al., 2012). RGL3 in particular mediates cross-talk between GA and JA pathways (Hou et al., 2013; Wild and Achard, 2013). JA selectively upregulate *RGL3,* whose product binds to JAZ repressors of JA signaling to boost the immune response at the expense of growth (Wild et al., 2012; Wild and Achard, 2013).

JA antagonism of growth and flowering

Our data raise the interesting possibility JA antagonism of GA conditions *bop1-6D* and *pny pnf* phenotypic defects. GO analysis of differentially regulated genes in the *bop1-6D* transcriptome revealed significant enrichment of terms related to stress stimuli including response to jasmonic acid stimulus and to a lesser extent reponses to salicylic acid, ethylene, and abscissic acid stimuli leading to the model that *BOP1* overexpression reprioritizes the plant for defense at the expense of growth. Higher levels of JA biosynthetic gene transcripts and hormone are found in *bop1-6D* and *pny pnf* apices relative to wild-type control plants. These data support the findings of Canet et al. (2012) who identified BOP1/2 as essential for MeJA-induced in priming for resistance to *Pseudomonas syringae* pv tomato DC3000. Plants exposed to high levels of jasmonate are stunted in growth of roots, leaves, and stems (Ellis et al., 2002; Cipollini, 2005; Bonaventure et al., 2007; Hyun et al., 2008; Zhang and Turner, 2008; Heinrich et al., 2013). Arabidopsis plants treated with jasmonate are also late flowering with short internodes and loss of apical dominance giving an appearance similar to *bop1-6D* or *pny pnf*/+ mutants. Inhibitory effects of MeJA on flowering are also reported in *Pharbitis nil* (Maciejewska and Kopceiwicz, 2002; Maciejewska et al., 2004), *Chenopodium rubrum* (Albrechtova and Ullmann, 1994) and wheat (Diallo et al., 2014). JA antagonism of growth or flowering has been linked to repression of GA biosynthesis (Heinrich et al., 2013; Magome et al., 2004), stabilization of DELLAs (Yang et al., 2012) and/or induction of AP2/ERF factors (Magome et al., 2008; Sun et al., 2008; Kang et al., 2011; Licausi et al., 2013). These data are consistent with JA contributing to *bop1-6D* and *pny pnf* developmental defects. Whilst inactivation of jasmonate biosynthesis by mutation of allene oxide synthase fails to rescue flowering in *pny pnf* mutants, a small but significant increase in plant height and flowering time in *bop1-6D* supports this model.

Our data suggest that resources in *pny pnf* are reallocated toward defense at the expense of flowering and provide evidence for JA as a factor in modulating growth and meristem activity at boundaries.

MATERIALS AND METHODS

Plant Material and Growth Conditions

In the Hepworth lab, Arabidopsis (*Arabidopsis thaliana*) plants were grown on soil or *in vitro* on AT minimal media (Haughn and Somerville, 1986) in growth chambers at 21°C under

572 continuous light (24h light, intensity 100 μmol m^{-2} s^{-1}), LD (16h light), or SD (8h light)
573 conditions. In the Pautot lab, plants were grown in LD (16h light:150 μmol m^{-2} s^{-1}) or SD (10
574 h light:1h at 80 μmol m^{-2} s^{-1}, 8 h at 130 μmol m^{-2} s^{-1},1h at 80 μmol m^{-2} s^{-1}) conditions. Wild-
575 type was the Col-0 ecotype of Arabidopsis. Mutant lines were obtained from the Arabidopsis
576 Biological Resource Center (https://abrc.osu.edu/) or Nottingham Arabidopsis Stock Centre
577 (http://nasc.nott.ac.uk). The *pny-40126* (SALK_40126), *pnf-96116* (SALK_96116), *bop1-3*
578 (SALK_012994), *bop2-1* SALK_075879), *knat6-1* (SALK_047931), *knat6-2*
579 (SALK_054482), *knat2-5* (SALK_099837), *ath1-1* (GABI-KAT_114A12), *ath1-3*
580 (SALK_113353) mutants have been described previously (Smith and Hake, 2003; Smith et
581 al., 2004; Hepworth et al., 2005; Belles-Boix et al., 2006; Proveniers et al., 2007; Gómez-
582 Mena and Sablowski, 2008). The *ath1-4* mutant was a gift from Lin Xu (Li et al., 2012).
583 *35S:BOP2* and *bop1-6D* overexpression lines were described previously (Norberg et al.,
584 2005). The *BOP1:GUS* and *BOP2:GUS* reporter lines were described previously (McKim et
585 al., 2008; Xu et al., 2010). The *35S:KNAT6* overexpression line was also described previously
586 (Shi et al., 2011).

587 **Plant genetics**

588 Primers and strategies used for genotyping *bop1-3*, *bop2-1, knat6-2* (Khan et al., 2012b), *pny-*
589 *40126* (Smith and Hake, 2003), *pnf-96116, pnf-33879* (Smith et al., 2004), *knat6-1, knat2-5*
590 (Ragni et al., 2008), *ath1-1* (Proveniers et al., 2007), *ath1-3* (Gòmez-Mena and Sablowski,
591 2008) have been previously described. For genotyping *ath1-4*, primers ath1-4dCAPS-F and
592 ath1-4dCAPS-R were used to amplify a 198-bp product from genomic DNA. Only the *ath1-4*
593 product is cleaved by SspI to yield a 173-bp fragment. All mutant combinations were
594 generated by crossing and confirmed by PCR genotyping. Primers are listed in Supplemental
595 Table S2.

596 **Phenotypic analyses**

597 For quantitative analysis of meristem arrest, seedlings were germinated on agar plates under
598 SDs, transferred to soil on Day 10, and scored for meristem arrest on Day 25. Progenies from
599 a selfed *pny pnf*/+ plant (n=624) and a selfed *knat2 pny pnf*/+ plant (n=146) were analyzed in
600 parallel with wild-type plants and *bop1 bop2 pny pnf*, *ath1 pny pnf*, and *knat6 pny pnf*
601 mutants (n=144). Quantitative analyses of inflorescence phenotypes were performed with 8-
602 week-old plants grown under LDs. Average height, internode length, and rosette paraclade

number were determined for ten plants per genotype as previously described (Ragni et al., 2008). Flowering time was scored for at least twenty-four plants per genotype by monitoring date of apex emergence since *bop1 bop2* mutants initiate leaves at a reduced rate (Norberg et al., 2005). Seeds were germinated directly on soil under LDs. All phenotypic analyses were performed at least twice under independent growth conditions with similar results.

In situ hybridization and localization of GUS activity

Plants for analysis were grown under SDs for three weeks followed by 15 days in continuous light prior to harvesting tissue. We used *in situ* hybridization to monitor gene expression since control sequences for expression of *KNAT2:GUS* and *KNAT6:GUS* reporters in inflorescence meristems are missing (Khan et al., 2012b). Tissue fixation, embedding, and sectioning were carried out as described (Nikovics et al., 2006) with minor changes. Hybridization was performed overnight using the following buffer: 50% formamide, 10% Dextran sulfate, 1X Denhardts, 0.3M NaCl, 10 mM Tris HCl pH 8, 1 mM EDTA, and 5 mg per ml of tRNA. Primers used to make *KNAT6*, *KNAT2*, *BOP2,* and *ATH1* antisense probes were as listed in Supplemental Table S2.

Tissues were analyzed for *BOP1:GUS* activity as described (Sieburth and Meyerowitz, 1997) with minor changes. Stained tissues were embedded in Paraplast Plus (Sigma) processed using tert-butanol instead of xylenes. Sections (10 μm) were cut from embedded tissue, affixed to glass slides, and dewaxed with tert-butanol prior to imaging.

Construction of *D35S:BOP1-GR, BOP1p-BOP1-GR, D35S:ATH1*, and *ATH1p:GUS* transgenic lines

A translational fusion of BOP1 to the steroid-binding domain of the rat glucocorticoid receptor was generated. Treatment with dexamethasone (DEX) leads to translocation of the GR fusion protein from the cytoplasm to the nucleus as a way of controlling transcription factor activity (Lloyd et al., 1994). The *BOP1* coding sequence lacking a stop codon was fused in-frame to the GR-fragment using overlap extension mutagenesis (Heckman and Pease, 2007). The resulting product was cloned into pCR-BluntII-TOPO (Invitrogen) to create B359. For all cloning steps involving amplification by PCR, iProof was used as the polymerase (BioRad) and cloned inserts were sequenced to ensure fidelity.

To create *D35S:BOP1-GR*, the *BOP1-GR* fusion gene present in B359 was amplified by PCR using CDS-BOP1-F and GR-R as the primers. The resulting product was modified to contain dATP overhangs and transferred to the Gateway-compatible entry vector pCR8/GW/TOPO (Invitrogen). LR clonase© (Invitrogen) was used to move the insert to a pSM-3 based destination vector containing a double 35S CaMV promoter (*D35S*) and Nos terminator (Carl Douglas lab, unpublished). Wild-type plants were transformed by floral dipping (Clough and Bent, 1998) using the Agrobacterium strain C58C1 pGV3101 pMP90 (Koncz and Schell, 1986). Hygromycin-resistant primary transformants were selected on agar plates containing 10 μm DEX. After transfer to soil, plants were sprayed daily with 10 μm DEX to induce nuclear localization of the BOP1-GR fusion protein. Homozygous progeny from one DEX-induced *D35S:BOP1-GR* line with a dwarf phenotype (line 9) was used for all subsequent experiments.

The *D35S:BOP1-GR* transgene failed to complement *bop1 bop2* plants, presumably because the *35S CaMV* promoter fails to provide the correct range of tissue expression. To confirm activity of the fusion protein and for use in ChIP experiments, the *BOP1-GR* fusion gene was expressed under control of the *BOP1* native promoter in *bop1 bop2* plants. The transgene was created in two steps. The *BOP1* promoter present in *pBOP1:GUS* (McKim et al., 2008) was amplified by PCR using primers 4H-4kb-EcoR1-F1 and 4H-4kb-Xma1-R1 that incorporated restriction sites at their 5' ends. The resulting product was digested with *Eco*R1 and *Xma*I and cloned into the corresponding sites of the binary vector pBAR (a gift from the Dangl Lab, University of North Carolina) to create B149. The *BOP1-GR* fusion gene present in B359 was amplified by PCR using primers Xma1-BOP1-F and BOP1-Xma1-R. The resulting product was digested with *Xma*I and cloned into the corresponding site of B149 to create pBAR/BOP1prom:BOP1-GR. The transgene was introduced into *bop1 bop2* plants by floral dipping. Primary transformants resistant to glufosinate-ammonium were selected on soil using the herbicide FINALE® (Farnam Companies). Three independent lines were used to assess complementation of *bop1 bop2* mutant phenotypes. T2 seeds were sown on agar plates containing phosphinothricin with/without 5 μm DEX. Plants were transferred to soil and sprayed daily with Mock or DEX solution until maturity. Complementation of leaf, floral patterning, and floral-organ abscission was observed in all DEX-treated lines (Supplemental Fig. S7).

To make the *D35S:ATH1* transgene, *ATH1* coding sequence was amplified by PCR from cloned cDNA template using ATH1-CDS-F1 and ATH1-CDS-F1 as the primers. The

665 resulting fragment was cloned into the entry vector pCR8/GW/TOPO and transferred into the
666 pSM-3 based destination vector as described above. Wild-type plants were transformed by
667 floral dipping. Transformants were selected on agar plates containing hygromycin.
668 Phenotypes were scored in the T1 generation.

669 To create *ATH1* promoter fusions to a GUS reporter gene, fragments containing 3.3-kb or 2-
670 kb of sequence upstream of the *ATH1* translation start site were amplified by PCR from
671 genomic DNA template (BAC MSD21) and fused to the coding region of the *uidA* gene
672 (GUS). Primers incorporating *Bam*HI and *Nco*I restriction sites at their 5' ends facilitated
673 directional cloning. Products were cloned into pCR-BluntII-TOPO for propagation. Inserts
674 were released by digestion with *Bam*HI and *Nco*I and ligated into the corresponding sites of
675 pGCO:GUS (Hepworth et al., 2002). Agrobacterium was co-transformed with pSOUP
676 (Hellens et al., 2000). Wild-type plants were transformed by floral dipping and glufosinate-
677 ammonium resistant primary transformants were selected on soil. Cloning primers are listed
678 in Supplemental Table S2.

679 **ChIP experiments**

680 ChIP was performed as described (Chakravarthy et al., 2003) using an anti-GR antibody
681 (Santa Cruz Biotechnology, Catalog # 1002) and Mock or DEX-treated *BOP1p:BOP1-GR*
682 *bop1 bop2* plants grown under LDs. Seeds were germinated on agar plates containing
683 phosphinothricin with or without 10 µm DEX. After transfer to soil, plants were sprayed daily
684 with Mock (0.04% ethanol) or DEX solutions. Leaf tissue was collected from 4-week-old
685 flowering plants for analysis. Quantification of immunoprecipitated DNA by RT-PCR was
686 performed as previously described (Boyle et al., 2009). Primers were as listed in
687 Supplemental Table S3.

688 **Microarray experimental design, hybridization, and analysis**

689 Tissue for profiling was harvested from the first expanded internodes of wild-type and *bop1-*
690 *6D* flowering plants grown under continuous light. RNA was extracted from four biological
691 replicates per genotype using an RNeasy Plant Mini Kit (Qiagen). The mRNA was amplified
692 according to the protocol described in the MessageAmp aRNA kit (Ambion, Catalog# 1750).
693 To produce incorporated antisense mRNA, aminoallyl-UTP was incorporated into the newly
694 synthesized aRNA; 3 µl of aminoallyl-UTP (50 mM) plus 2 µl of UTP (75 mM) instead of 4
695 µl of UTP were added during the aRNA amplification. Labelling, hybridization, and scanning

were performed as described (Xiang et al., 2011). To normalize for bias in dye labelling, two biological replicates were labelled with Cy3 and two were labelled with Cy5. Experiments were carried out using Arabidopsis 70-mer oligo microarray slides (http://ag.arizona.edu/microarray). Two colour microarray data were pre-preprocessed with the marray package (Yang et al., 2009) implemented in R/BioConductor (R Development Core Team, 2011; (Gentleman et al., 2004) using the background correction method "normexp" (offset=50) and the normalize within arrays method "loess". Differentially expressed genes were identified by p-values and fold change and by contrasts using linear models for microarrays (Smyth, 2005) and included a dye effect assessment implemented in R/BioConductor.

qRT-PCR

Total RNA was isolated using Trizol reagent (Invitrogen) from dissected apices of wild-type and mutants. Plants grown under SDs were harvested on Day 25 (SD) or transferred to LDs to induce flowering and harvested after 12 days (LD). Dissected apices were <0.5 cm tall with the majority of surrounding leaves >0.2 cm removed. Tissues were collected in the subjective afternoon for all samples (after 9 – 12 hrs of light in a 16 hour cycle). cDNA was generated using 1 μg of RNA as the template under following conditions: Step 1: 70 ^{o}C for 5 min; Step 2: 50 ^{o}C for 60 mins and Step 3: 70 ^{o}C for 15 mins. qRT-PCR was carried out as described (Khan et al. 2012b) with the following changes. Reactions in triplicate containing 2 µl of 10-fold diluted cDNA, except for *LFY* and *AP1* reactions which required 4 µl of diluted cDNA, gene-specific primers (Supplemental Table S3), and POWER SYBR Green PCR mastermix (Invitrogen) were carried out using a StepOnePlus Thermocycler (Applied Biosystems). *GAPC* was used as a normalization control. Quantification of *miR156* mRNA was performed as described (Porri et al., 2012). Data shown are the average of three biological replicates conducted using separate growth trials and independently isolated RNA samples. Error bars, s.e.m.

For DEX induction experiments, total RNA was prepared from internodes of 4-week-old flowering plants expressing the *D35S:BOP1-GR* transgene. Internodes were harvested from primary and secondary inflorescences of 5-6 plants starting at the bottom above the first silique and all the way up to where internodes were too small to collect. Tissue was excised with a new razor blade on parafilm, frozen in liquid nitrogen, and stored at -80°C until further analysis. Plants were treated continuously with Mock (0.12% ethanol), 30 µm DEX, 50 µm

728 cycloheximide (CHX), or 30 µm DEX + 50 µm CHX for 2, 4, or 24 hours by inverting
729 inflorescences into containers of solution. For long-term treatments, seedlings were
730 germinated on agar plates containing 10 µm DEX. After transplanting to soil, plants were
731 sprayed daily with a solution of Mock (0.04% ethanol) or DEX for four weeks until tissue
732 was harvested for RNA extraction. Values were normalized to *EIF4A1* transcript (At3g13920)
733 and then to the Mock control for DEX treatments, and to the CHX control for DEX+CHX
734 treatments to correct for negative effects of CHX on the transcription of *BOP1* target genes
735 (Jun et al., 2010; Nakamichi et al., 2010). Data shown are the average of three biological
736 replicates conducted using independently isolated RNA samples. Error bars, s.e.m.

737 **Hormone treatments**

738 To analyze the effect of GA on growth, ten-day-old seedlings grown under continuous light
739 were sprayed daily with GA (100 µm GA_3, 0.02% Silwett L-77) or a Mock (0.02% Silwett L-
740 77) solution until maturity (Hay et al., 2002). To examine the effect of JA on growth, seven-
741 day-old seedlings grown under LDs were sprayed daily with MeJA (100 µm MeJA, 0.02%
742 Silwett L-77) or a Mock (0.02% Silwett L-77) solution until maturity (Canet et al., 2012).
743 MeJA-treated plants were covered with a plastic dome for 1 hour following treatments and
744 solutions were made fresh once a week. Flowering time was determined by scoring the date of
745 apex emergence. At least 24 plants per genotype were monitored.

746 **JA measurements**

747 For measurement of JA, wild-type, *bop1 bop2*, and *bop1-6D* plants were grown for 6 to 7
748 weeks under LDs. Pools of 30 apices (buds+ internodes) were used for each replicate (100 mg
749 of fresh material). Wild-type and *pny pnf* plants were grown for 4 weeks under SDs. Pools of
750 30 apices (90 mg of fresh material) were used for each replicate. Three biological replicates
751 were collected for each condition. Tissues were directly harvested in liquid nitrogen. Tissues
752 were ground in liquid nitrogen and lyophilized. For each sample, 10 mg of freeze-dried
753 powder were extracted with 0.8 mL of acetone/water/acetic acid (80/19/1 v:v:v) containing 2
754 ng of [5-2H] jasmonic acid (CDN Isotopes CIL Cluzeau, Sainte Foy la Grande, France) (Le
755 Roux et al., 2014). The extract was vigorously shaken for 1 min, sonicated for 1 min at 25 Hz,
756 shaken for 10 minutes at 4°C in a Thermomixer (Eppendorf), and then centrifuged (8,000xg,
757 4 °C, 10 min). The supernatants were collected, and the pellets were re-extracted twice with
758 0.4 mL of the same extraction solution, then vigorously shaken (1 min) and sonicated (1 min;

25 Hz). After the centrifugations, the three supernatants were pooled and dried (final volume 1.6 mL). Each dry extract was dissolved in 140 µL of acetonitrile/water (50/50 v/v), filtered, and analyzed using a Waters Acquity ultra performance liquid chromatograph coupled to a Waters Xevo Triple quadrupole mass spectrometer TQS (UPLC-ESI-MS/MS). The compounds were separated on a reverse-phase column (Uptisphere C18 UP3HDO, 100*2.1 mm*3µm particle size; Interchim, France) using a flow rate of 0.4 mL min^{-1} and a binary gradient: (A) acetic acid 0.1 % in water (v/v) and (B) acetonitrile with 0.1 % acetic acid. For jasmonic acid, the following binary gradient (t, % A): (0 min., 98 %), (3 min., 70 %), (7.5 min., 50 %), (8.5 min., 5 %), (9.6 min., 0%), (13.2 min., 98 %), (15.7 min., 98 %) was used. Mass spectrometry was conducted in electrospray and Multiple Reaction Monitoring scanning mode (MRM mode) in negative ion mode. Relevant instrumental parameters were set as follows: capillary 1.5 kV (negative mode), source block and desolvation gas temperatures 130 °C and 500 °C, respectively. Nitrogen was used to assist the cone and desolvation (150 L h^{-1} and 800 L h^{-1}, respectively). Argon was used as the collision gas at a flow of 0.18 mL/min. The parameters used for MRM quantification of JA are described in (Le Roux et al., 2014). Samples were reconstituted in 140 µL of 50/50 acetonitrile/H_2O (v/v) *per* mL of injected volume. The JA limit of detection (LOD) and limit of quantification (LOQ) were extrapolated from calibration curves and samples using the Quantify module of MassLynx software (version 4.1). The amount of JA was expressed as a ratio of peak areas (209>62/214>62) per dry weight due to impurities contained in the D5-JA standard.

Accession Numbers

Sequence data from this article can be found in the EMBL/GenBank data libraries under accession numbers At1g70510 (*KNAT2*), At1g23380 (*KNAT6*), At5g02030 (*PNY*), At2g27990 (*PNF*), At3g57130 (*BOP1*), At2g41370 (*BOP2*), At4g32980 (*ATH1*)

Supplemental Data

The following supplemental materials are available.

Supplemental Figure S1. Ectopic expression of *KNAT6* and *ATH1* mimics *pny* and *pny pnf*/+ phenotype.

Supplemental Figure S2. *ATH1* map and characterization of mutant alleles.

Supplemental Figure S3. Phenotypes of other mutant combinations.

Supplemental Figure S4. Quantitative phenotypic analyses of *bop1 bop2 pny pnf*, *ath1 pny pnf* and *knat6 pny pnf* mutants.

Supplemental Figure S5. *BOP1:GUS* expression in Col and *pny pnf* apices.

Supplemental Figure S6. *BOP2*, *ATH1*, *KNAT2*, and *KNAT6* expression in *pny* and *pnf* apices.

Supplemental Figure S7. Complementation of *bop1 bop2* mutant by *BOP1p::BOP1-GR* construct.

Supplemental Table S1. Gene ontology classification of differentially expressed genes in *bop1-6D* versus Col internode microarrays.

Supplemental Table S2. List of general primers.

Supplemental Table S3. List of primers for qRT-PCR.

ACKNOWLEDGMENTS

We thank the Salk Institute Genomic Analysis Laboratory for providing the sequence-indexed Arabidopsis T-DNA insertion mutants. We thank Hervé Ferry and Bruno Letarnec for greenhouse management. We thank Gregory Mouille and the IJPB Green Chemistry Platform for the quantification of jasmonic acid. Laura Ragni was supported by the European Marie-Curie (FP6) Program. We thank Alex Edwards for *BOP1p::BOP1-GR bop1 bop2* complementation data and Jin Cheong/Mike Bush for constructing the *bop1 bop2 pny pnf* quadruple mutant. Brenda Chisanga was supported by a Douglas Anglin Scholarship. Madiha Khan was supported in part by a Women in Science award from L'Oréal Canada and the France-Canada Research Fund. This paper is dedicated to the memory of Jean-Pierre Rullière.

AUTHOR CONTRIBUTIONS

All authors made essential contributions to the project. M.K., L.R., P.T., and B.C.S. performed most of the experiments. J.L. analyzed the *ATH1p:GUS* lines. S.C., C.Y., D.X., and R.D. provided the microarray data. X.K. and C.D. performed the ChIP assays. H.M. performed the *in situ* analysis with V.P. S.C. measured JA content and provided technical assistance to V.P. J-P.R. provided technical assistance to V.P. M.P. participated by communicating unpublished results. S.R.H. and V.P. conceived the project, designed the experiments, did some of the experiments, analyzed the data, and wrote the article.

FIGURE LEGENDS

Figure 1. Inactivation of *BOP1/2*, *ATH1*, and *KNAT6* rescue *pny pnf* meristem arrest. Plants were grown under SDs. Number of plants showing a meristem arrest on Day 25 indicated at top right of panels. A, Col plant. The SAM produces leaves. B, *pny pnf* mutant showing a meristem arrest. 90/156 (57.7%) of expected *pny pnf* mutants in a *pny pnf*/+ segregating population (n=624) showed SAM arrest (arrow). C, *knat2 pny pnf* triple mutant; identical to *pny pnf* mutant. 11/36.5 (30.1%) of expected *knat2 pny pnf* triple mutants in a *knat2 pny pnf*/+ segregating population (n=146) showed SAM arrest (arrow). D, *ath1 pny pnf* triple mutant; no meristem arrest. E, *bop1 bop2 pny pnf* quadruple mutant; no meristem arrest. F, *knat6 pny pnf* triple mutant; no meristem arrest. Scale bars = 5 mm.

Figure 2. Inactivation of *BOP1/2*, *ATH1* and *KNAT6* rescues internode and flower formation in *pny pnf* mutants. Representative 8-week-old plants are shown. A, Col plant. B, *pnf* mutant showing a wild-type phenotype. C, *pny* mutant showing partial loss of apical dominance, short stature, and clusters of siliques. D, *pny pnf*/+ hemi mutant showing partial loss of apical dominance, short stature, clusters of siliques, and stem/pedicel fusion defects (see also Supplemental Fig. 1). E, *pny pnf* double mutant; non-flowering. F, *bop1 bop2 pny pnf* quadruple mutant; similar to *bop1 bop2*. Inactivation of *BOP1* and *BOP2* in *pny pnf* rescues internode elongation and flowering. G, *ath1 pny pnf* triple mutant; similar to *ath1*. Inactivation of *ATH1* in *pny pnf* rescues internode elongation and flowering. H, *knat6 pny pnf* mutant; similar to wild-type. Inactivation of *KNAT6* in *pny pnf* rescues internode elongation and flowering. I, *knat2 pny pnf* mutant; identical to *pny pnf* mutant. Scale bars = 2 cm.

Figure 3. *BOP2*, *ATH1*, *KNAT2,* and *KNAT6* expression in *pny pnf* apices. Plants were grown for 3 weeks under SDs and transferred to continuous light to induce flowering. Apices were harvested on Day 15. Transcript accumulation was monitored by *in situ* hybridization using longitudinal sections of Col (A, B, C, D) and *pny pnf* (E, F, G, H) apices and gene-specific probes. IM, inflorescence meristem. Numbers in panels indicate stage of floral development (Smyth et al., 1990). A, Col apex showing *BOP2* expression in floral meristems (until stage 2) and in the boundary domains of older flowers (late stage 2 and stage 3 are shown). B, Col apex showing *ATH1* expression in an incipient floral primordium and the dome of a stage 2 flower. C, Col apex showing *KNAT2* transcripts localized to boundary domains flanking the IM and older flowers. Expression is also observed in floral primordia and the dome of stage 2 flowers. D, Col apex showing *KNAT6* transcripts localized to boundary domains flanking the IM and in a stage 3 flower. E-H, *pny pnf* apices showing expanded expression of *BOP2* (E),

854 *ATH1* (F), *KNAT2* (G) and *KNAT6* (H) in the central and rib zones of the meristem. Scale bars
855 = 40 μm.

856 **Figure 4.** Activation of *ATH1* and *KNAT6* in DEX-induced *D35S:BOP1-GR* line. A, Col
857 plant. B, *bop1-6D* mutant with shortened internodes and clustered siliques. C-D, *D35S:BOP1-*
858 *GR* plants treated with Mock or DEX solutions for four weeks. C, Mock-treated *D35S:BOP1-*
859 *GR* plant showing a wild-type phenotype. D, DEX-induced *D35S:BOP1-GR* plant showing a
860 phenotype similar to *bop1-6D* mutant. E, Comparison of *KNAT6* and *ATH1* transcript levels
861 in wild-type versus *bop1-6D* mutants and Mock versus DEX-induced *D35S:BOP1-GR* plants
862 after continuous treatment for four weeks. F, Comparison of *KNAT6* and *ATH1* transcript
863 levels in DEX-induced *D35S:BOP1-GR* lines with and without protein synthesis inhibitor
864 cycloheximide (CHX). Transcripts were measured after 2 and 4 hours of treatment. Scale bars
865 = 2 cm.

866 **Figure 5.** Identification of the genomic region responsible for *ATH1* induction by BOP1. A-
867 H, Functional characterization of the *ATH1* regulatory region. Representative expression
868 patterns are shown for *D35S:BOP1-GR* plants containing 2-kb (A, C, E, G) or 3.3-kb (B, D,
869 F, H) *ATH1p:GUS* reporter genes as diagrammed in (I). Promoter activity was monitored by
870 GUS staining after incubation of 10-day-old seedlings or 6-week-old inflorescences for 4
871 hours in Mock or 30 μm DEX solutions. Comparison of Mock (A-D) and DEX (E-H) panels
872 shows that expression is upregulated in the leaves, flowers, and the stem of DEX-induced
873 lines for both promoter constructs. Scale bars = 1 mm. I, Map of the *ATH1* promoter and 5'
874 untranslated region. Closed arrowhead mark the 5' end of genomic fragments used in
875 construction of 2-kb and 3.3-kb *ATH1p:GUS* reporter genes. Predicted consensus binding
876 sites for TGA bZIP factors (Schindler, 1992; Izawa et al., 1993; Fode et al., 2008) are shown
877 in relation to fragments amplified by qRT-PCR after ChIP to test for BOP1 localization
878 (horizontal bars). Sites in red (IV and VII) contain A-boxes and show enrichment for BOP1.
879 J, Quantification of BOP1-GR enrichment at sites IV and VII in the *ATH1* promoter by qRT-
880 PCR. Anti-GR ChIP was performed using leaves from Mock and DEX-treated *35S:BOP1-GR*
881 *bop1 bop2* plants. Fold-enrichment at sites IV and VII is presented as the ratio of DEX versus
882 Mock transcript levels after normalization to the unrelated *UBQ5* control sequence. Three
883 biological replicates were quantified to show enrichment at Site IV. One biological replicate
884 was quantified to show enrichment at Site VII. Three technical replicates were performed for
885 each. Error bars, s.d.

886 **Figure 6.** Quantification of flowering time and meristem-identity transcripts in wild-type and
887 mutants. A, Quantitative analysis of flowering-time. Plants were grown under LDs. Date of
888 apex emergence for *bop1 bop2 pny pnf*, *knat6 pny pnf*, and *ath1 pny pnf* mutants is
889 comparable to wild-type with minor variations. Lines containing *ath1* flowered slightly earlier
890 (-6.7 days) and lines containing *bop1 bop2* flowered slightly later (+3.1 days) than wild-type.
891 Asterisks indicate significant differences (Student's *t* test, $p<0.01$). B, Quantitative analysis of
892 meristem identity gene expression. Flowering was induced by shifting plants from SDs to
893 LDs. Apices were harvested on Day 37 at the end of 12 LDs. Inflorescence meristem-identity
894 gene transcripts *SOC1* and *FUL* are expressed at similar levels in Col and *pny pnf* apices.
895 Floral meristem-identity gene transcripts *FD*, *LFY*, *AP1*, and *CAL* are significantly lower in
896 *pny pnf* compared to Col apices. Transcript accumulation resumes in *bop1 bop2 pny pnf*,
897 *knat6 pny pnf*, *ath1 pny pnf* apices. C, Quantitative analysis of *miR156* and *SPL* transcript
898 abundance in wild-type and mutant apices. Non-flowering in *pny pnf* correlates with a
899 significant increase in *miR156* abundance at the expense of *SPL3,4,6,9,* and *15* transcripts
900 relative to Col plants. Transcript accumulation in *bop1 bop2 pny pnf*, *knat6 pny pnf*, *ath1 pny*
901 *pnf* mutants follows a pattern similar to wild-type, consistent with restored flowering.
902 Asterisks in B and C indicate significant differences (Student's *t* test, $p<0.05$).

903 **Figure 7.** *BOP1* overexpression mimics *pny pnf* defects in *SPL* transcript accumulation and
904 GA homeostasis. Plants were grown in continuous light. qRT-PCR was used to assess
905 transcript accumulation in apices and/or internodes. A, Accumulation of *miR156* and *SPL*
906 transcripts in Col and *bop1-6D* internodes. B, Schematic representation of non-13-
907 hydroxylated GA biosynthetic and catabolic pathways in Arabidopsis (Hu et al., 2008;
908 Yamaguchi, 2008). Green lettering, GA biosynthetic enzymes monitored for transcript
909 accumulation in C, D. Red lettering, GA catabolic enzyme monitored for transcript
910 accumulation in C, D. Bioactive GA_4 in bold. Inactive GA metabolites shown on right.
911 GGDP, geranylgeranyl diphosphate; CDP, *ent*-copalyl diphosphate; CPS, *ent*-copalyl
912 diphosphate synthase; KS, *ent*-kaurene synthase; KO, *ent*-kaurene oxidase; KAO, *ent*-
913 kaurenoic acid oxidase. C and D, Accumulation of GA pathway transcripts in *pny pnf* apices
914 and *bop1-6D* apices and internodes. E, *pny pnf* and *bop1-6D* plants treated with 100 μm GA_3
915 or a Mock solution. F, Flowering time and plant height of Col and *bop1-6D* plants treated
916 with 100 μm GA_3 or a Mock solution. Asterisks in A, C, and D indicate significant
917 differences (Student's *t* test, $p<0.05$).

Figure 8. Transcript profiling of floral repressor genes in *bop1-6D* and *pny pnf* mutants. A, Floral repressor genes differentially expressed in *bop1-6D* compared to Col internodes according to microarray experiment (see Materials and Methods). B, Repressor transcript profile of *bop1-6D* and *pny pny* mutants quantified by qRT-PCR. No differential expression was observed for *FLC* transcript. Transcripts encoding AP2-like TOE2 and SMZ repressors and AP2/ERF TINY, DDF1, and DDF2 repressors were differentially upregulated in agreement with (A). Asterisks indicate significant differences (Student's *t* test, $p<0.05$).

Figure 9. *BOP1* overexpression increases JA content by transcriptional upregulation of biosynthetic genes. A, JA-related genes differentially expressed in *bop1-6D* compared to Col internodes identified by microarray experiment (Materials and Methods). B, Schematic representation of JA biosynthetic pathway in Arabidopsis (Park et al., 2002; Wasternak and Hause, 2013). Red lettering, transcripts investigated by qRT-PCR in (C). Linolenic acid is released from membrane lipids by a lipolytic enzyme (DAD1/DEFECTIVE IN ANTHER DEHISCENCE1) and converted to allene oxide (12,13-epoxy-octadecantrienoic acid) by lipoxygenase (LOX) and allene oxide synthase (AOS). One cyclization, one reduction, and three rounds of β-oxidation steps are required in producing jasmonic acid (JA) which is conjugated to isoleucine (JA-Ile) in bioactive form (Wasternak and Kombrink, 2010). DAD1, DEFECTIVE IN ANTHER DEHISCENCE1; AOS, allene oxidase synthase; LOX, lipooxygenase; AOC, allene oxide cyclase; OPR3/DDE1, 12-oxo-phytodienoic acid-10,11-reductase3/DELAYED DEHISCENCE1; ACX, Acetyl-CoA oxidase; MPF, multifunctional protein; KAT, L-3-ketoacyl CoA thiolase; JAR1, JASMONATE RESISTANT1. C, Quantitative analysis of JA biosynthetic gene transcripts in *bop1-6D* and *pny pnf* mutants grown under SDs or LDs. Asterisks indicate significant differences (Student's *t* test, $p<0.05$). D, Concentration of JA in wild-type tissues compared to *bop1-6D*, *bop1 bop2*, and *pny pnf* mutants (see Materials and Methods).

Figure 10. Effect of loss or gain of JA content on phenotype of wild-type and mutants. A-G, Wild-type and *pny* plants were sprayed daily until maturity with 100 μm MeJA or a Mock solution. A, Mock-treated Col plant. B, MeJA-treated Col plant showing small, dark green leaves. C, *bop1-6D* mutant showing a compact rosette similar to (B). D, JA-treated Col plants showing *pny*-like partial loss of apical dominance and short stature. E, JA-treated *pny* mutant showing enhancement of defects in internode elongation and apical dominance relative to Mock control (see G). F, JA-treated *pny* mutant showing delayed flowering relative to Mock control. G, Quantitative phenotypic analysis of wild-type and *pny* mutant plants treated with MeJA. Plants were grown under LDs. For both genotypes, treatment with MeJA resulted in additional rosette paraclades indicating loss of apical dominance, reduced height, and delayed flowering. Asterisks indicate significant differences (Student's *t* test, $p<0.05$). H-J, Effect of *aos* loss-of-function on *pny pnf* and *bop1-6D* phenotypes. Representative plants are shown. H, *pny pnf aos* mutant remains non-flowering. I-J, Phenotype of *bop1-6D* versus *bop1-6D aos* mutants. A small but highly significant ($p<0.0001$) increase in plant height (+1.26 cm) and earlier flowering (-1.8 days) is measured in *bop1-6D aos* compared to *bop1-6D* control plants. Analysis was performed in a *bop1-6D/+ aos/+* segregating population (n=100). Scale bars = 1.5 cm.

Figure 11. Summary and model. PNY-PNF/STM limit expression of *BOP1/2* and downstream effectors *ATH1/KNAT6* to boundary domains flanking the IM. BOP1 acting via an unknown TGA bZIP co-factor directly activates *ATH1* whereas promotion of *KNAT6* is indirect (red arrow). These products form a module that represses growth, meristem activity, and flowering by increasing JA content via transcriptional promotion of JA biosynthetic genes. Either directly or indirectly (dashed lines), we propose that misexpression of this pathway leads to down-regulation of GA pathway components and repression of the *miR156-SPL-miR172* module at one or more nodes in correlation with increased content of associated classes of floral repressors (e.g. DELLA, AP2-like, and AP2/ERF clades). Ultimately, *SPL* and *FD/FT* transcripts (not depicted) fail to accumulate and activation of floral meristem identity genes *LFY*, *AP1*, and *CAL* required for flower initiation is blocked. Internode elongation is also blocked.

975 **LITERATURE CITED**

976 **Abe M, Kobayashi Y, Yamamoto S, Daimon Y, Yamaguchi A, Ikeda Y, Ichinoki H,**
977 **Notaguchi M, Goto K, Araki T** (2005) FD, a bZIP protein mediating signals from
978 the floral pathway integrator FT at the shoot apex. Science **309:** 1052-1056
979 **Aichinger E, Kornet N, Friedrich T, Laux T** (2012) Plant stem cell niches. Annu Rev Plant
980 Biol **63:** 615-636
981 **Aida M, Tasaka M** (2006) Genetic control of shoot organ boundaries. Curr Opin Plant Biol
982 **9:** 72-77
983 **Albrechtová J, Ullmann J** (1994) Methyl jasmonate inhibits growth and flowering in
984 *Chenopodium rubrum*. Biol Plantarum **36:** 317-319
985 **Amasino RM, Michaels SD** (2010) The timing of flowering. Plant Physiol **154:** 516-520
986 **Andrés F, Coupland G** (2012) The genetic basis of flowering responses to seasonal cues.
987 Nat Rev Genet **13:** 627-639
988 **Andrés F, Romera-Branchat M, Martínez-Gallegos R, Patel V, Schneeberger K, Jang S,**
989 **Altmüller J, Nürnberg P, Coupland G** (2015) Floral induction in Arabidopsis
990 thaliana by FLOWERING LOCUS T requires direct repression of BLADE-ON-
991 PETIOLE genes by homeobox protein PENNYWISE. Plant Physiol, this issue
992 **Aukerman M, Sakai H** (2003) Regulation of flowering time and floral organ identity by a
993 microRNA and its APETALA2-like target genes. Plant Cell **15:** 2730-2741
994 **Belles-Boix E, Hamant O, Witiak SM, Morin H, Traas J, Pautot V** (2006) *KNAT6*: an
995 Arabidopsis homeobox gene involved in meristem activity and organ separation. Plant
996 Cell **18:** 1900-1907
997 **Bernier G** (1988) The control of floral evocation and morphogenesis. Annu Rev Plant
998 Physiol **39:** 175-219
999 **Bonaventure G, Gfeller A, Proebsting WM, Hörsteiner S, Chételat A, Martinoia E,**
1000 **Farmer EE** (2007) A gain-of-function allele of TPC1 activates oxylipin biogenesis
1001 after leaf wounding in Arabidopsis. Plant J **49:** 899-898
1002 **Bowman J, Alvarez J, Weigel D, Meyerowitz E** (1993) Control of flower development in
1003 *Arabidopsis thaliana* by *APETALA1* and interacting genes. Development **119:** 721-
1004 743
1005 **Boyle P, Le Su E, Rochon A, Shearer HL, Murmu J, Chu JY, Fobert PR, Després C**
1006 (2009) The BTB/POZ domain of the Arabidopsis disease resistance protein NPR1

1007 interacts with the repression domain of TGA2 to negate its function. Plant Cell **21:**
1008 3700-3713
1009 **Byrne ME, Barley R, Curtis M, Arroyo JM, Dunham M, Hudson A, Martienssen RA**
1010 (2000) *Asymmetric leaves1* mediates leaf patterning and stem cell function in
1011 Arabidopsis. Nature **408:** 967-971
1012 **Byrne ME, Groover AT, Fontana JR, Martienssen RA** (2003) Phyllotactic pattern and
1013 stem cell fate are determined by the Arabidopsis homeobox gene *BELLRINGER*.
1014 Development **130:** 3941-3950
1015 **Canet J, Dobón A, Fajmonová J, Tornero P** (2012) The *BLADE-ON-PETIOLE* genes of
1016 Arabidopsis are essential for resistance induced by methyl jasmonate. BMC Plant Biol
1017 **12:** 199
1018 **Chakravarthy S, Tuori RP, D'Ascenzo MD, Fobert PR, Després C, Martin GB** (2003)
1019 The tomato transcription factor Pti4 regulates defense-related gene expression via
1020 GCC box and non-GCC box *cis* elements. Plant Cell **15:** 3033-3050
1021 **Cho S, Coruh C, Axtell M** (2012) miR156 and miR360 regulate tasiRNA accumulation and
1022 developmental timing in *Physcomitrella patens*. Plant Cell **24:** 4837-4849
1023 **Cipollini D** (2005) Interactive effects of lateral shading and jasmonic acid on morphology,
1024 phenology, seed production,and defense traits in *Arabidopsis thaliana*. Int J Plant Sci
1025 **166:** 955-959
1026 **Clark SE, Jacobsen SE, Levin JZ, Meyerowitz EM** (1996) The *CLAVATA* and *SHOOT*
1027 *MERISTEMLESS* loci competitively regulate meristem activity in Arabidopsis.
1028 Development **122:** 1567-1575
1029 **Clough SJ, Bent AF** (1998) Floral dip: a simplified method for *Agrobacterium*-mediated
1030 transformation of *Arabidopsis thaliana*. Plant J **16:** 735-743
1031 **Corbesier L, Vincent C, Jang S, Fornara F, Fan Q, Searle I, Giakountis A, Farrona S,**
1032 **Gissot L, Turnbull C, Coupland G** (2007) FT protein movement contributes to long-
1033 distance signaling in floral induction of Arabidopsis. Science **316:** 1030-1033
1034 **Cui L-G, Shan J-X, Shi M, Gao J-P, Lin H-X** (2014) The *miR156-SPL9-DFR* pathway
1035 coordinates the relationship between development and abiotic stress tolerance in
1036 plants. Plant J **80:** 1108-1117
1037 **Després C, DeLong C, Glaze S, Liu E, Fobert PR** (2000) The Arabidopsis NPR1/NIM1
1038 protein enhances the DNA binding activity of a subgroup of the TGA family of bZIP
1039 transcription factors. Plant Cell **12:** 279-290

1040 **Diallo A, Agharbaoui Z, Badawi M, Ali-Benali M, Moheb A, Houde M, Sarhan F** (2014)
1041 Transcriptome analysis of an *mvp* mutant reveals important changes in global gene
1042 expression and a role for methyl jasmonate in vernalization and flowering in wheat. J
1043 Exp Bot **65:** 2271-2286
1044 **Dill A, Thomas S, Hu J, Steber C, Sun T-P** (2004) The Arabidopsis F-box protein
1045 SLEEPY1 targets gibberellin signaling repressors for gibberellin-induced degradation.
1046 Plant Cell **16:** 1392-1405
1047 **Ellis C, I. K, Wasternak C, Turner JG** (2002) The Arabidopsis mutant *cev1* links cell wall
1048 signaling to jasmonate and ethylene responses. Plant Cell **14:** 1557-1566
1049 **Endrizzi K, Moussian B, Haecker A, Levin JZ, Laux T** (1996) The *SHOOT*
1050 *MERISTEMLESS* gene is required for maintenance of undifferentiated cells in
1051 Arabidopsis shoot and floral meristems and acts at a different regulatory level than the
1052 meristem genes *WUSCHEL* and *ZWILLE*. Plant J **10:** 967-979
1053 **Eriksson S, Bohlenius H, Moritz T, Nilsson O** (2006) GA_4 is the active gibberellin in the
1054 regulation of *LEAFY* transcription and Arabidopsis floral initiation. Plant Cell **18:**
1055 2171-2181
1056 **Etchells J, Moore L, Jiang WZ, Prescott H, Capper R, Saunders NJ, Bhatt AM,**
1057 **Dickinson HG** (2012) A role for *BELLRINGER* in cell wall development is supported
1058 by loss-of-function phenotypes. BMC Plant Biol **12:** 212
1059 **Fode B, Siemsen T, Thurow C, R W, Gatz C** (2008) The Arabidopsis GRAS protein SCL14
1060 interacts with class II TGA transcription factors and is essential for the activation of
1061 stress-inducible promoters. Plant Cell **20:** 3122-3135
1062 **Galvão V, Horrer D, Küttner F, Schmid M** (2012) Spatial control of flowering by DELLA
1063 proteins in *Arabidopsis thaliana*. Development **139:** 4072-4082
1064 **Gentleman RC, Carey VJ, Bates DM, Bolstad B, Dettling M, Dudoit S, Ellis B, Gautier**
1065 **L, Ge Y, Gentry J, Hornik K, Hothorn T, Huber W, Iacus S, Irizarry R, Leisch**
1066 **F, Li C, Maechler M, Rossini AJ, Sawitzki G, Smith C, Smyth G, Tierney L,**
1067 **Yang JY, Zhang J** (2004) Bioconductor: open software development for
1068 computational biology and bioinformatics. Genome Biol **5:** R80
1069 **Gómez-Mena C, Sablowski R** (2008) *ARABIDOPSIS THALIANA HOMEOBOX GENE1*
1070 establishes the basal boundaries of shoot organs and controls stem growth. Plant Cell
1071 **20:** 2059-2072

1072 **Ha CM, Jun JH, Nam HG, Fletcher JC** (2007) BLADE-ON-PETIOLE 1 and 2 control
1073 Arabidopsis lateral organ fate through regulation of LOB domain and adaxial-abaxial
1074 polarity genes. Plant Cell **19:** 1809-1825
1075 **Hamama L, Naouar A, Gala R, Voisine L, Pierre S, Jeauffre J, Cesbron D, Leplat F,**
1076 **Foucher F, Dorion N, Hibrand-Saint Oyant L** (2012) Overexpression of the
1077 RoDELLA impacts the height, branching, and flowering behaviour of *Pelargonium* X
1078 *domesticum* transgenic plants. Plant Cell Rep **31:** 2015-2029
1079 **Hamant O, Pautot V** (2010) Plant development: a TALE story. CR Biol **333:** 371-381
1080 **Haughn GW, Somerville C** (1986) Sulfonylurea-resistant mutants of *Arabidopsis thaliana*.
1081 Mol Gen Genet **204:** 430-434
1082 **Hay A, Kaur H, Phillips A, Hedden P, Hake S, Tsiantis M** (2002) The gibberellin pathway
1083 mediates KNOTTED1-type homeobox function in plants with different body plans.
1084 Curr Biol **12:** 1557-1565
1085 **Hay A, Tsiantis M** (2010) KNOX genes: versatile regulators of plant development and
1086 diversity. Development **137:** 3153-3165
1087 **Heckman KL, Pease LR** (2007) Gene splicing and mutagenesis by PCR-driven overlap
1088 extension. Nat Protoc **2:** 924-932
1089 **Heinrich M, Hettenhausen C, Lange T, Wunsche H, Fang J, Baldwin I, Wu J** (2013)
1090 High levels of jasmonic acid antagonize the biosynthesis of gibberellins and inhibit the
1091 growth of *Nicotiana attenuata* stems. Plant J **73:** 591-606
1092 **Hellens RP, Edwards EA, Leyland NR, Bean S, Mullineaux PM** (2000) pGreen: a
1093 versatile and flexible binary Ti vector for *Agrobacterium*-mediated plant
1094 transformation. Plant Mol Biol **42:** 819-832
1095 **Hepworth SR, Valverde F, Ravenscroft D, Mouradov A, Coupland G** (2002) Antagonistic
1096 regulation of flowering-time gene *SOC1* by CONSTANS and FLC via separate
1097 promoter motifs. EMBO J **21:** 4327-4337
1098 **Hepworth SR, Zhang Y, McKim S, Li X, Haughn GW** (2005) BLADE-ON-PETIOLE-
1099 dependent signaling controls leaf and floral patterning in Arabidopsis. Plant Cell **17:**
1100 1434-1448
1101 **Hou X, Ding L, Yu H** (2013) Crosstalk between GA and JA signaling mediates plant growth
1102 and defense. Plant Cell Rep **32:** 1067-1074
1103 **Hu J, Mitchum M, Barnaby N, Ayele B, Ogawa M, Nam E, Lai W-C, Hanada A, Alonso**
1104 **J, Ecker J, Swain S, Yamaguchi S, Kamiya Y, Sun T-P** (2008) Potential sites of

bioactive gibberellin production during reproductive growth in Arabidopsis. Plant Cell **20:** 320-336

Huijser P, Schmid M (2011) The control of developmental phase transitions in plants. Development **138:** 4117-4129

Hyun Y, Choi S, Hwang H-J, Yu J, Nam S-J, Ko J, Park J-Y, Seo YS, Kim EY, Ryu SB, Kim WT, Lee YH, Kang H, Lee I (2008) Cooperation and functional diversification of two closely related galactolipase genes for jasmonate biosynthesis. Dev Cell **14:** 183-192

Izawa T, Foster R, Chua N-H (1993) Plant bZIP protein DNA binding specificity. J Mol Biol **230:** 1131-1144

Jaeger KE, Wigge PA (2007) FT protein acts as a long-range signal in Arabidopsis. Curr Biol **17:** 1050-1054

Jun JH, Ha CM, Fletcher JC (2010) BLADE-ON-PETIOLE1 coordinates organ determinacy and axial polarity in arabidopsis by directly activating ASYMMETRIC LEAVES2. Plant Cell **22:** 62-76

Jung J-H, Seo Y-H, Seo P, Reyes J, Yun J, Chua N-H, Park C-M (2007) The *GIGANTEA*-regulated miRNA172 mediates photoperiodic flowering independent of *CONSTANS* in Arabidopsis. Plant Cell **19:** 2736-2748

Jung JH, Ju Y, Seo PJ, Lee JH, Park CM (2012) The SOC1-SPL module integrates photoperiod and gibberellic acid signals to control flowering time in Arabidopsis. Plant J **69:** 577-588

Kang H-G, Kim J, Kim B, Jeong H, Choi SH, Kim EK, Lee H-Y, Lim PO (2011) Overexpression of *FTL1/DDF1*, an AP2 transcription factor, enhances tolerance to cold, drought, and heat stresses in *Arabidopsis thaliana*. Plant Sci **180:** 634-641

Kanrar S, Bhattacharya M, Arthur B, Courtier J, Smith HMS (2008) Regulatory networks that function to specify flower meristems require the function of homeobox genes PENNYWISE and POUND-FOOLISH in Arabidopsis. Plant J **54:** 924-937

Kanrar S, Onguka O, Smith HMS (2006) Arabidopsis inflorescence architecture requires the activities of KNOX-BELL homeodomain heterodimers. Planta **224:** 1163-1173

Kardailsky I, Shukla VK, Ahn JH, Dagenais N, Christensen SK, Nguyen JT, Chory J, Harrison MJ, Weigel D (1999) Activation tagging of the floral inducer *FT*. Science **286:** 1962-1965

Khan M, Tabb P, Hepworth SR (2012a) *BLADE-ON-PETIOLE1* and *2* regulate Arabidopsis inflorescence architecture in conjunction with homeobox genes *KNAT6* and *ATH1*. Plant Signal Behav **7:** 788-792

Khan M, Xu H, Hepworth SR (2014) *BLADE-ON-PETIOLE* genes: setting boundaries in development and defense. Plant Sci **215-216:** 157-171

Khan M, Xu M, Murmu J, Tabb P, Liu Y, Storey K, McKim SM, Douglas CJ, Hepworth SR (2012b) Antagonistic interaction of BLADE-ON-PETIOLE1 and 2 with BREVIPEDICELLUS and PENNYWISE regulates Arabidopsis inflorescence architecture. Plant Physiol **158:** 946-960

Kim J, Lee JH, Kim W, Jung HS, Huijser P, Ahn JH (2012) The *microRNA156-SQUAMOSA PROMOTER BINDING PROTEIN-LIKE3* module regulates ambient temperature-responsive flowering via *FLOWERING LOCUS T* in Arabidopsis. Plant Physiol **159:** 461-478

Koncz C, Schell J (1986) The promoter of TL-DNA gene *5* controls the tissue-specific expression of chimeric genes carried by a novel type of *Agrobacterium* binary vector. Mol Gen Genet **204:** 383-396

Lal S, Pacis LB, Smith HM (2011) Regulation of the *SQUAMOSA PROMOTER-BINDING PROTEIN-LIKE genes/microRNA156* module by the homeodomain proteins PENNYWISE and POUND-FOOLISH in Arabidopsis. Mol Plant **4:** 1123-1132

Le Roux C, Del Prete S, Boutet-Mercey S, Perreau F, Balagué C, Roby D, Fagard M, Gaudin V (2014) The hnRNP-Q protein LIF2 participates in the plant immune response. PLoS One **9:** e99343

Li Y, Pi L, Huang H, Xu L (2012) ATH1 and KNAT2 proteins act together in regulation of plant inflorescence architecture. J Exp Bot **63:** 1423-1433

Licausi F, Ohme-Takagi M, Perata P (2013) APETALA2/Ethylene Responsive Factor (AP2/ERF) transcription factors: mediators of stress responses and developmental programs. New Phytol **199:** 639-649

Lincoln C, Long J, Yamaguchi J, Serikawa K, Hake S (1994) A *knotted1*-like homeobox gene in Arabidopsis is expressed in the vegetative meristem and dramatically alters leaf morphology when overexpressed in transgenic plants. Plant Cell **6:** 1859-1876

Lloyd AM, Schena M, Walbot V, Davis RW (1994) Epidermal cell fate determination in Arabidopsis: patterns defined by a steroid-inducible regulator. Science **266:** 436-439

Long JA, Moan EI, Medford JI, Barton MK (1996) A member of the KNOTTED class of homeodomain proteins encoded by the *STM* gene of Arabidopsis. Nature **379:** 66-69

Maciejewska B, Kopceiwicz J (2002) Inhibitory effect of methyl jasmonate on flowering and elongation growth in *Pharbitis nil*. J Plant Growth Regul **21:** 216-223

Maciejewska BD, Kesy J, Zielinska M, Kopcewicz J (2004) Jasmonates inhibit flowering in short-day plant *Pharbitis nil*. Plant Growth Regul **43:** 1-8

Magome H, Yamaguchi S, Hanada A, Kamiya Y, Oda K (2008) The DDF1 transcriptional activator upregulates expression of a gibberellin-deactivating gene, *GA2ox7*, under high-salinity stress in Arabidopsis. Plant J **56:** 613-626

Magome H, Yamguchi S, Hanada A, Kamiya Y, Oda K (2004) *Dwarf and delayed-flowering 1*, a novel Arabidopsis mutant deficient in gibberellin biosynthesis because of overexpression of a putative AP2 transcription factor. Plant J **37:** 720-729

Mathieu J, Warthmann N, Kuttner F, Schmid M (2007) Export of FT protein from phloem companion cells is sufficient for floral induction in Arabidopsis. Curr Biol **17:** 1055-1060

Mathieu J, Yant LJ, Murdter F, Kuttner F, Schmid M (2009) Repression of flowering by the miR172 target SMZ. PLoS Biol **7:** e1000148

Matsoukas I, Massiah AJ, Thomas B (2012) Florigenic and antiflorigenic signaling in plants. Plant Cell Physiol **53:** 1827-1842

McKim SM, Stenvik GE, Butenko MA, Kristiansen W, Cho SK, Hepworth SR, Aalen RB, Haughn GW (2008) The *BLADE-ON-PETIOLE* genes are essential for abscission zone formation in Arabidopsis. Development **135:** 1537-1546

Mele G, Ori N, Sato Y, Hake S (2003) The *knotted1*-like homeobox gene BREVIPEDICELLUS regulates cell differentiation by modulating metabolic pathways. Genes Dev **17:** 2088-2093

Mutasa-Göttgens E, Hedden P (2009) Gibberellin as a factor in floral regulatory networks. J Exp Bot **60:** 1979-1989

Nakamichi N, Kiba T, Henriques R, Mizuno T, Chua NH, Sakakibara H (2010) PSEUDO-RESPONSE REGULATORS 9, 7, and 5 are transcriptional repressors in the Arabidopsis circadian clock. Plant Cell **22:** 594-605

Navarro L, Bari R, Achard P, Lison P, Nemri A, Harberd NP, Jones JDG (2008) DELLAs control plant immune responses by modulating the balance of jasmonic acid and salicylic acid signaling. Curr. Biol. **16:** 650-655

Nikovics K, Blein T, Peaucelle A, Ishida T, Morin H, Aida M, Laufs P (2006) The balance between the *MIR164A* and *CUC2* genes controls leaf margin serration in Arabidopsis. Plant Cell **18:** 2929-2945

Norberg M, Holmlund M, Nilsson O (2005) The *BLADE ON PETIOLE* genes act redundantly to control the growth and development of lateral organs. Development **132:** 2203-2213

Park J-H, Halitschke R, Kim BH, Baldwin IT, Feldmann K, Feyereisen R (2002) A knock-out mutation in allene oxide synthase results in male sterility and defective wound signal transduction in Arabidopsis due to a block in jasmonic acid biosynthesis. Plant J **31:** 1-12

Peaucelle A, Louvet R, Johansen JN, Salsac F, Morin H, Fournet F, Belcram K, Gillet F, Höfte H, Laufs P, Mouille G, Pelloux J (2011) The transcription factor BELLRINGER modulates phyllotaxis by regulating the expression of a pectin methylesterase in Arabidopsis. Development **138:** 4733-4741

Porri A, Torti S, Romera-Branchat M, Coupland G (2012) Spatially distinct regulatory roles for gibberellins in the promotion of flowering of Arabidopsis under long photoperiods. Development **139:** 2198-2209

Proveniers M (2013) Sugars speed up the circle of life. eLife **2:** e00625

Proveniers M, Rutjens B, Brand M, Smeekens S (2007) The Arabidopsis TALE homeobox gene *ATH1* controls floral competency through positive regulation of *FLC*. Plant J **52:** 899-913

Ragni L, Belles-Boix E, Gunl M, Pautot V (2008) Interaction of *KNAT6* and *KNAT2* with *BREVIPEDICELLUS* and *PENNYWISE* in Arabidopsis inflorescences. Plant Cell **20:** 888-900

Rutjens B, Bao D, van Eck-Stouten E, Brand M, Smeekens S, Proveniers M (2009) Shoot apical meristem function in Arabidopsis requires the combined activities of three BEL1-like homeodomain proteins. Plant J **58:** 641-654

Schindler U, Beckman, H., and Cashmore, A.R. (1992) TGA1 and G-box binding factors: two distinct classes of Arabidopsis leucine zipper proteins compete for the G-box-like element TGACGTGG. Plant Cell **4:** 1309-1319

Shi CL, Stenvik GE, Vie AK, Bones AM, Pautot V, Proveniers M, Aalen RB, Butenko MA (2011) Arabidopsis class I KNOTTED-like homeobox proteins act downstream in the IDA-HAE/HSL2 floral abscission signaling pathway. Plant Cell **23:** 2553-2567

Sieburth LE, Meyerowitz EM (1997) Molecular dissection of the *AGAMOUS* control region shows that *cis* elements for spatial regulation are located intragenically. Plant Cell **9:** 355-365

Smith HM, Campbell BC, Hake S (2004) Competence to respond to floral inductive signals requires the homeobox genes *PENNYWISE* and *POUND-FOOLISH*. Curr Biol **14:** 812-817

Smith HM, Hake S (2003) The interaction of two homeobox genes, *BREVIPEDICELLUS* and *PENNYWISE*, regulates internode patterning in the Arabidopsis inflorescence. Plant Cell **15:** 1717-1727

Smith HM, Ung N, Lal S, Courtier J (2011) Specification of reproductive meristems requires the combined function of SHOOT MERISTEMLESS and floral integrators FLOWERING LOCUS T and FD during Arabidopsis inflorescence development. J Exp Bot **62:** 583-593

Smyth DR, Bowman JL, Meyerowitz EM (1990) Early flowering development in Arabidopsis. Plant Cell **2:** 755-767

Smyth GK (2005) Limma: linear models for microarray data. *In* RC Gentleman, VJ Carey, S Dudoit, R Irizarry, W Huber, eds, Bioinformatics and computational biology solutions using R and Bioconductor. Springer, New York, pp 397-420

Srikanth A, Schmid M (2011) Regulation of flowering time: all roads lead to Rome. Cell Mol Life Sci **68:** 2013-2037

Stief A, Altmann S, Hoffmann K, Pant BD, Scheible W-R, Bäurle I (2014) Arabidopsis miR156 regulates tolerance to recurring environmental stress through SPL transcription factors. Plant Cell **26:** 1792-1807

Sun S, Yu J-P, Chen F, Zhou T-J, Fang X-H, Li Y-Q, Sui S-F (2008) TINY, a dehydration-responsive element (DRE)-binding protein-like transcription factor connecting the DRE- and ethylene-responsive element-mediated signaling pathways in Arabidopsis. J Biol Chem **283:** 6261-6271

Teper-Bamnolker P, Samach A (2005) The flowering integrator FT regulates *SEPALLATA3* and *FRUITFULL* accumulation in Arabidopsis leaves. Plant Cell **17:** 2661-2675

Tian C, Zhang X, He J, Yu H, Wang Y, Shi B, Han Y, Wang G, Feng X, Zhang C, Wang J, Qi J, Yu R, Jiao Y (2014) An organ boundary-enriched gene regulatory network uncovers regulatory hierarchies underlying axillary meristem initiation. Mol Sys Biol **10:** 755

Ung N, Lal S, Smith HMS (2011a) The role of PENNYWISE and POUND-FOOLISH in the maintenance of the shoot apical meristem in Arabidopsis. Plant Physiol **156:** 605-614

Ung N, Smith HMS (2011b) Regulation of shoot meristem integrity during Arabidopsis vegetative development. Plant Signal Behav **6:** 1250-1252

Wang J-W, Czech, B, Weigel D (2009) miR156-regulated SPL transcription factors define an endogenous flowering pathway in *Arabidopsis thaliana*. Cell **138:** 738-739

Wang JW (2014) Regulation of flowering time by the miR156-mediated age pathway. J Exp Bot **65:** 4723-4730

Wasternak C, Hause B (2013) Jasmonates: biosynthesis, perception, signal transduction and action in plant stress response, growth and development. An update to the 2007 review in Annals of Botany. Ann Bot **111:** 1021-1058

Wasternak C, Kombrink E (2010) Jasmonates: structural requirements for lipid-derived signals active in plant stress responses and development. ACS Chem Biol **5:** 63-77

Wigge PA, Kim MC, Jaeger KE, Busch W, Schmid M, Lohmann JU, Weigel D (2005) Integration of spatial and temporal information during floral induction in Arabidopsis. Science **309:** 1056-1059

Wild M, Achard P (2013) The DELLA protein RGL3 positively contributes to jasmonate/ethylene defense responses. Plant Signal Behav **8:** e23891

Wild M, Davière JM, Cheminant S, Regnault T, Baumberger N, Heintz D, Baltz R, Genschik P, Achard P (2012) The Arabidopsis DELLA *RGA-LIKE3* is a direct target of MYC2 and modulates jasmonate signaling responses. Plant Cell **24:** 3307-3319

Wu G, Park M, Conway S, Wang J-W, Weigel D, Poethig RS (2009) The sequential action of miR156 and miR172 regulates developmental timing in Arabidopsis. Cell **138:** 750-759

Wu G, Poethig RS (2006) Temporal regulation of shoot development in *Arabidopsis thaliana* by *miR156* and its target *SPL3*. Development **133:** 3539-3547

Xiang D, Venglat P, Tibiche C, Yang H, Risseeuw E, Cao Y, Babic V, Cloutier M, Keller W, Wang E, Selvaraj G, Datla R (2011) Genome-wide analysis reveals gene expression and metabolic network dynamics during embryo development in Arabidopsis. Plant Physiol **156:** 346-356

Xu M, Hu T, McKim SM, Murmu J, Haughn GW, Hepworth SR (2010) Arabidopsis BLADE-ON-PETIOLE1 and 2 promote floral meristem fate and determinacy in a previously undefined pathway targeting APETALA1 and AGAMOUS-LIKE24. Plant J **63:** 974-989

Yamaguchi A, Wu MF, Yang L, Wu G, Poethig RS, Wagner D (2009) The microRNA-regulated SBP-Box transcription factor SPL3 is a direct upstream activator of *LEAFY*, *FRUITFULL*, and *APETALA1*. Dev Cell **17:** 268-278

1305 **Yamaguchi S** (2008) Gibberellin metabolism and its regulation. Annu Rev Plant Biol **59:**
1306 225-251
1307 **Yang D-L, Yao J, Mei C-S, Tong X-H, Zeng L-J, Li Q, Xiao L-T, Sun T, Li J., Deng X-**
1308 **W, Lee CM, Thomashow MF, Yang Y., He Z, He SY** (2012) Plant hormone
1309 jasmonate prioritizes defense over growth by interfering with gibberellin signaling
1310 cascade. Proc Natl Acad Sci USA **109:** 1192-2000
1311 **Yang L, Xu M, Koo Y, He J, Poethig RS** (2013) Sugar promotes vegetative phase change in
1312 *Arabidopsis thaliana* by repressing the expression of *MIR156A* and *MIR156C*. eLife
1313 **2:** e00260
1314 **Yang Y, Paquet A, Dudoit S** (2009) Package 'marray': exploratory analysis for two-color
1315 spotted microarray data. Version 1.42.0.
1316 **Yant L, Mathieu J, Dinh TT, Ott F, Lanz C, Wollmann H, Chen X, Schmid M** (2010)
1317 Orchestration of the floral transition and floral development in Arabidopsis by the
1318 bifunctional transcription factor APETALA2. Plant Cell **22:** 2156-2170
1319 **Yu S, Cao L, Zhou C-M, Zhang T-Q, Lian H, Sun Y, Wu J, Huang J, Wang G, Wang J-**
1320 **W** (2013) Sugar is an endogenous cue for juvenile-to-adult phase transition in plants.
1321 eLife **2:** e00269
1322 **Yu S, Galvão VC, Zhang YC, Horrer D, Zhang TQ, Hao YH, Feng YQ, Wang S,**
1323 **Schmid M, Wang JW** (2012) Gibberellin regulates the Arabidopsis floral transition
1324 through miR156-targeted SQUAMOSA promoter binding-like transcription factors.
1325 Plant Cell **24:** 3320-3332
1326 **Zhang Y, Turner JG** (2008) Wound-induced endogenous jasmonates stunt plant growth by
1327 inhibiting mitosis. PLoS One **3:** e3699
1328 **Zhao M, Yang S, Chen C-Y, Li C, Shan W, Lu W, Cui Y, Liu X, K W** (2015) Arabidopsis
1329 BREVIPEDICELLUS interacts with the SWI2/SNF2 chromatin remodeling ATPase
1330 BRAHMA to regulate *KNAT2* and *KNAT6* expression in control of inflorescence
1331 architecture. PLoS Genet **11:** e1005125
1332 **Zhu Q-H, Helliwell CA** (2011) Regulation of flowering time and floral patterning by
1333 miR172. J Exp Bot **62:** 487-495
1334

1335

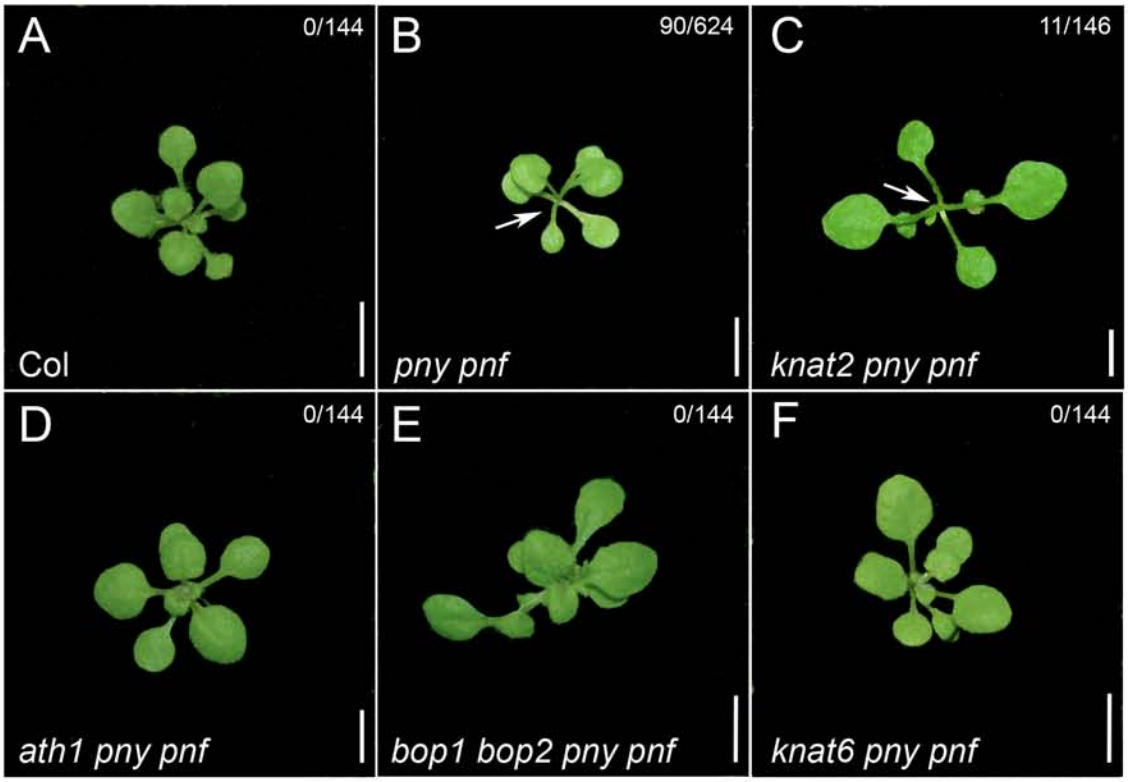

Figure 1. Inactivation of *BOP1/2*, *ATH1*, and *KNAT6* rescue *pny pnf* meristem arrest. Plants were grown under SDs. Number of plants showing a meristem arrest on Day 25 indicated at top right of panels. A, Col plant. The SAM produces leaves. B, *pny pnf* mutant showing a meristem arrest. 90/156 (57.7%) of expected *pny pnf* mutants in a *pny pnf*/+ segregating population (n=624) showed SAM arrest (arrow). C, *knat2 pny pnf* triple mutant; identical to *pny pnf* mutant. 11/36.5 (30.1%) of expected *knat2 pny pnf* triple mutants in a *knat2 pny pnf*/+ segregating population (n=146) showed SAM arrest (arrow). D, *ath1 pny pnf* triple mutant; no meristem arrest. E, *bop1 bop2 pny pnf* quadruple mutant; no meristem arrest. F, *knat6 pny pnf* triple mutant; no meristem arrest. Scale bars = 5 mm.

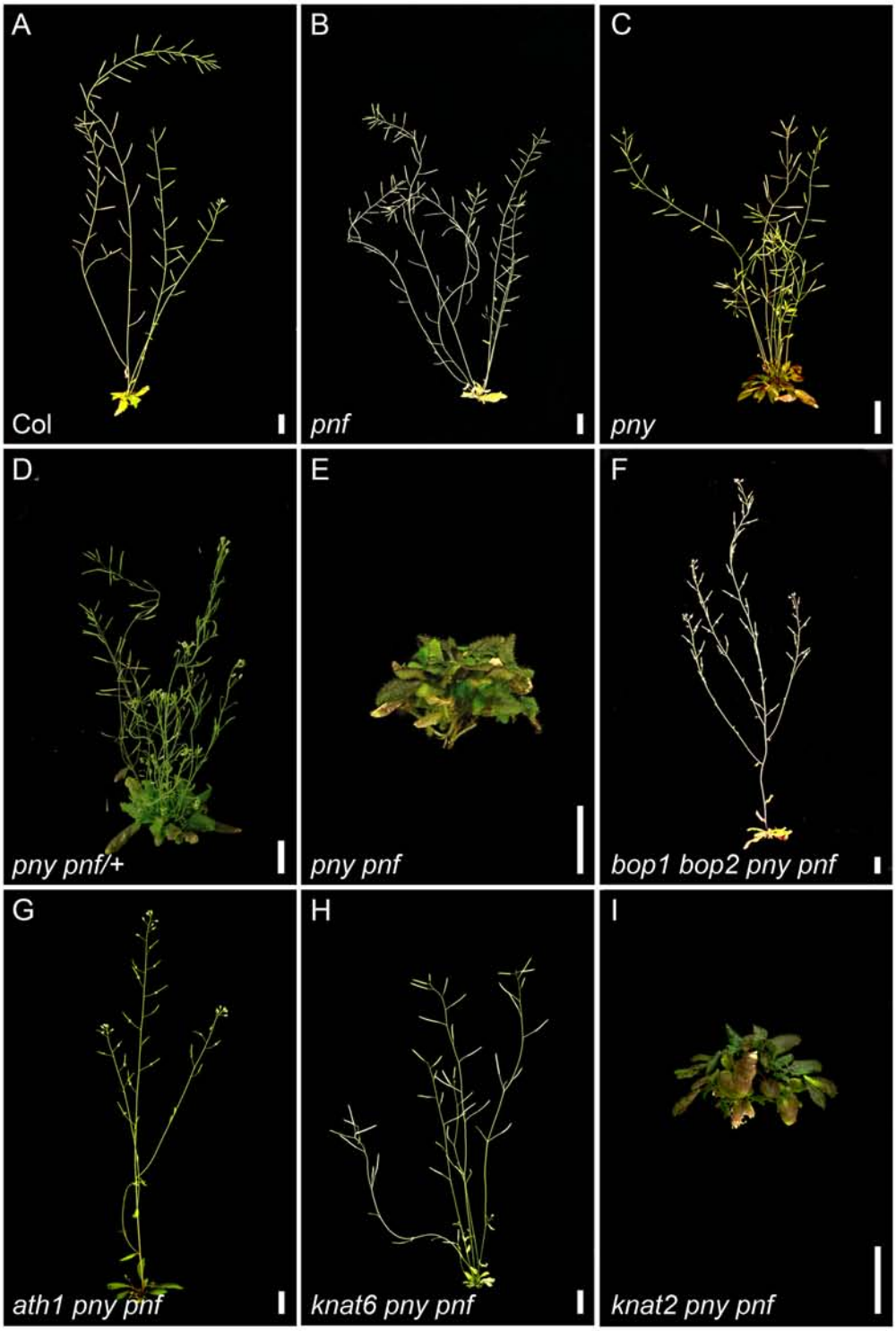

Figure 2. Inactivation of *BOP1/2, ATH1* and *KNAT6* rescues internode and flower formation in *pny pnf* mutants. Representative 8-week-old plants are shown. A, Col plant. B, *pnf* mutant showing a wild-type phenotype. C, *pny* mutant showing partial loss of apical dominance, short stature, and clusters of siliques. D, *pny pnf/+* hemi mutant showing partial loss of apical dominance, short stature, clusters of siliques, and stem/pedicel fusion defects (see also Supplemental Fig. 1). E, *pny pnf* double mutant; non-flowering. F, *bop1 bop2 pny pnf* quadruple mutant; similar to *bop1 bop2*. Inactivation of *BOP1* and *BOP2* in *pny pnf* rescues internode elongation and flowering. G, *ath1 pny pnf* triple mutant; similar to *ath1*. Inactivation of *ATH1* in *pny pnf* rescues internode elongation and flowering. H, *knat6 pny pnf* mutant; similar to wild-type. Inactivation of *KNAT6* in *pny pnf* rescues internode elongation and flowering. I, *knat2 pny pnf* mutant, identical to *pny pnf* mutant. Scale bars = 2 cm.

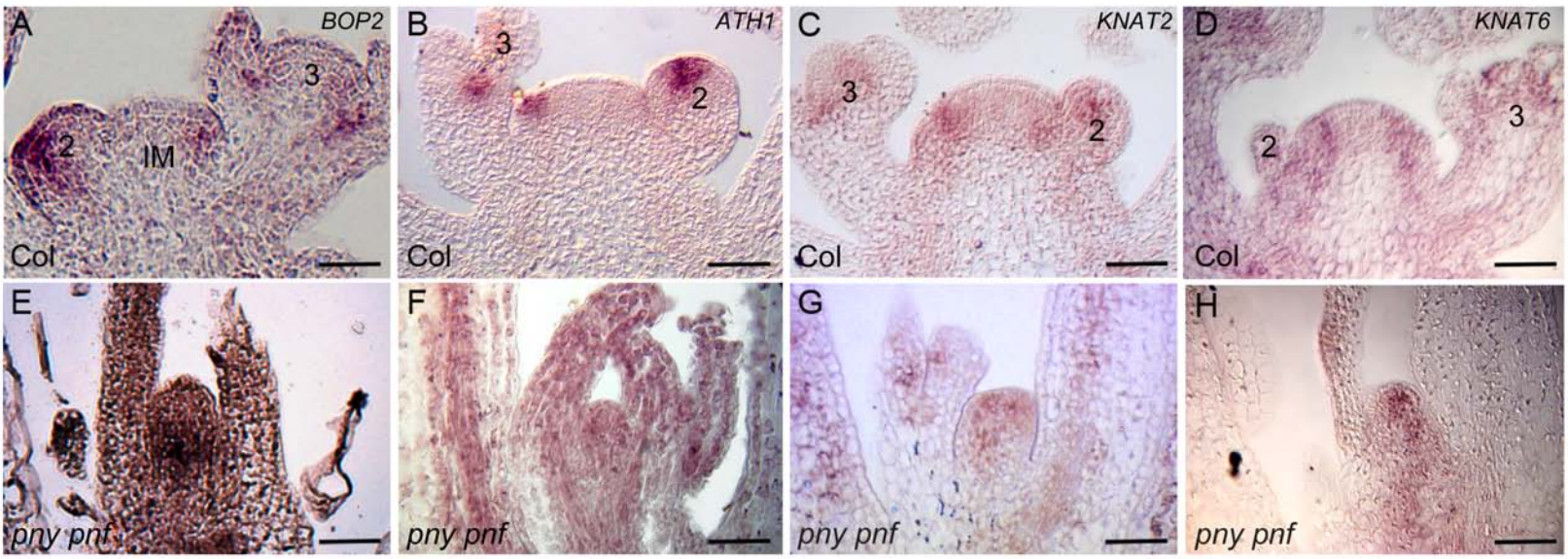

Figure 3. *BOP2*, *ATH1*, *KNAT2*, and *KNAT6* expression in *pny pnf* apices. Plants were grown for 3 weeks under SDs and transferred to continuous light to induce flowering. Apices were harvested on Day 15. Transcript accumulation was monitored by *in situ* hybridization using longitudinal sections of Col (A, B, C, D) and *pny pnf* (E, F, G, H) apices and gene-specific probes. IM, inflorescence meristem. Numbers in panels indicate stage of floral development (Smyth et al., 1990). A, Col apex showing *BOP2* expression in floral meristems (until stage 2) and in the boundary domains of older flowers (late stage 2 and stage 3 are shown). B, Col apex showing *ATH1* expression in an incipient floral primordium and the dome of a stage 2 flower. C, Col apex showing *KNAT2* transcripts localized to boundary domains flanking the IM and older flowers. Expression is also observed in floral primordia and the dome of stage 2 flowers. D, Col apex showing *KNAT6* transcripts localized to boundary domains flanking the IM and in a stage 3 flower. E-H, *pny pnf* apices showing expanded expression of *BOP2* (E), *ATH1* (F), *KNAT2* (G) and *KNAT6* (H) in the central and rib zones of the meristem. Scale bars = 40 μm.

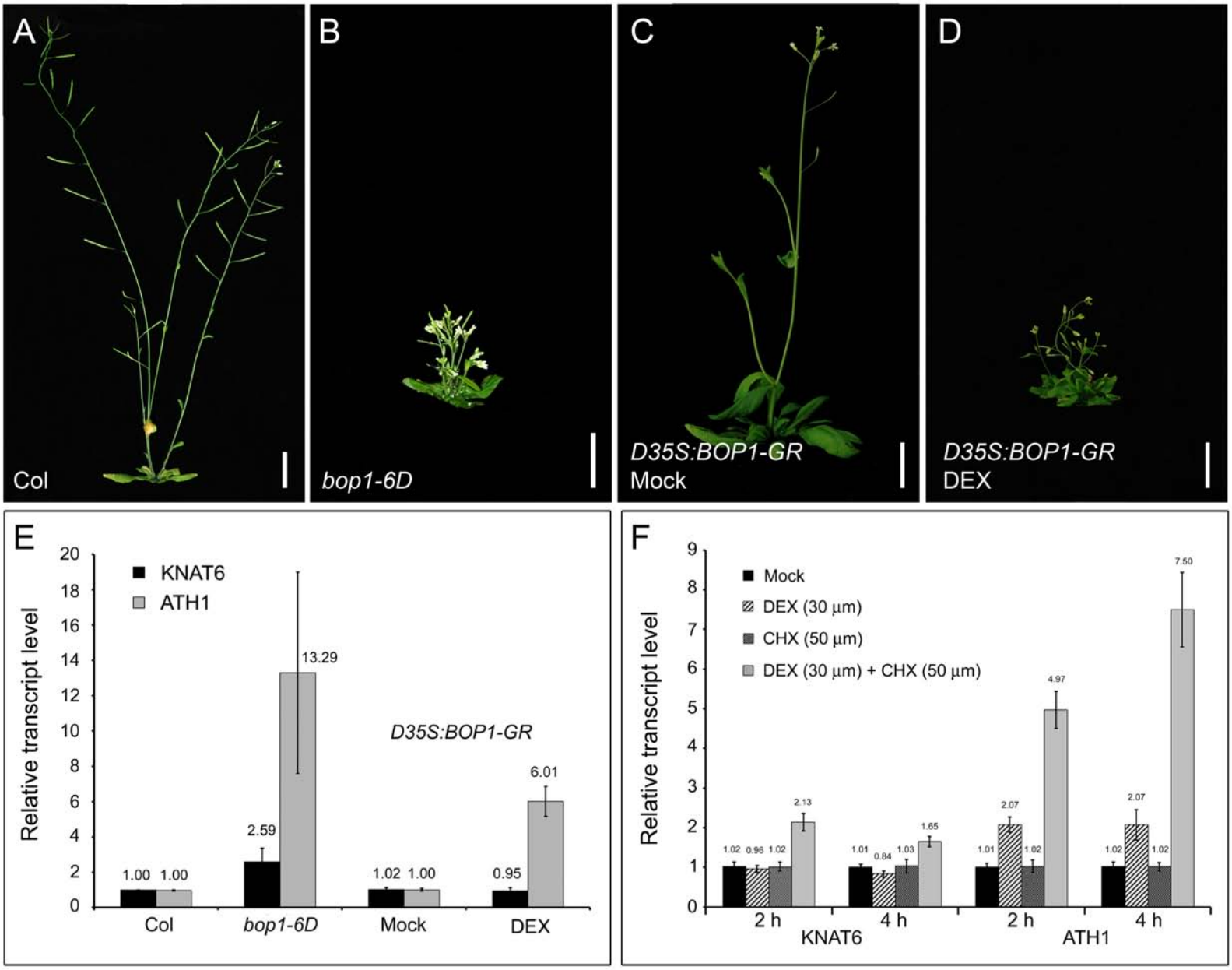

Figure 4. Activation of *ATH1* and *KNAT6* in DEX-induced *D35S:BOP1-GR* line. A, Col plant. B, *bop1-6D* mutant with shortened internodes and clustered siliques. C-D, *D35S:BOP1-GR* plants treated with Mock or DEX solutions for four weeks. C, Mock-treated *D35S:BOP1-GR* plant showing a wild-type phenotype. D, DEX-induced *D35S:BOP1-GR* plant showing a phenotype similar to *bop1-6D* mutant. E, Comparison of *KNAT6* and *ATH1* transcript levels in wild-type versus *bop1-6D* mutants and Mock versus DEX-induced *D35S:BOP1-GR* plants after continuous treatment for four weeks. F, Comparison of *KNAT6* and *ATH1* transcript levels in DEX-induced *D35S:BOP1-GR* lines with and without protein synthesis inhibitor cycloheximide (CHX). Transcripts were measured after 2 and 4 hours of treatment. Scale bars = 2 cm.

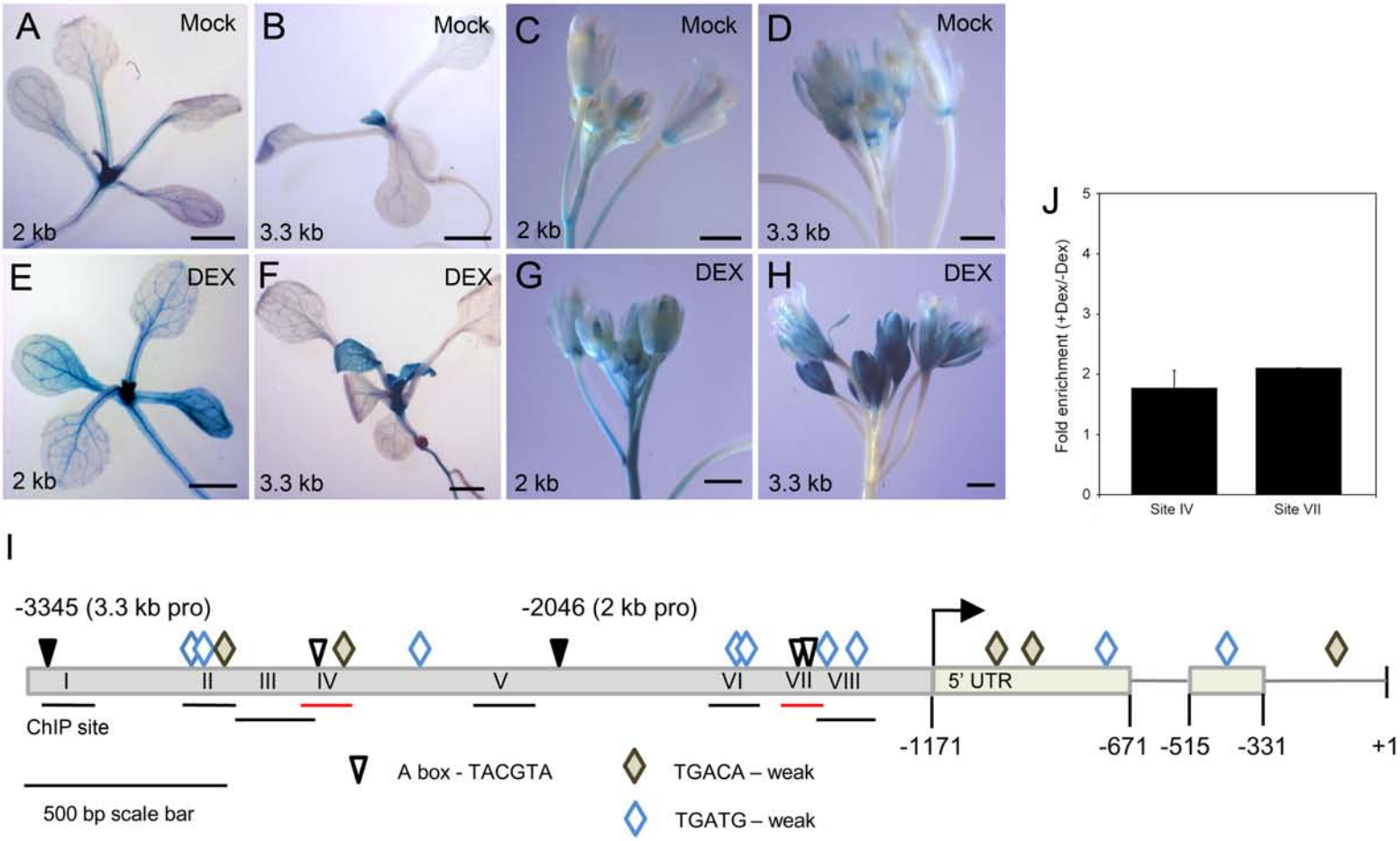

Figure 5. Identification of the genomic region responsible for *ATH1* induction by BOP1. A-H, Functional characterization of the *ATH1* regulatory region. Representative expression patterns are shown for *D35S:BOP1-GR* plants containing 2-kb (A, C, E, G) or 3.3-kb (B, D, F, H) *ATH1p:GUS* reporter genes as diagrammed in (I). Promoter activity was monitored by GUS staining after incubation of 10-day-old seedlings or 6-week-old inflorescences for 4 hours in Mock or 30 µm DEX solutions. Comparison of Mock (A-D) and DEX (E-H) panels shows that expression is upregulated in the leaves, flowers, and the stem of DEX-induced lines for both promoter constructs. Scale bars = 1 mm. I, Map of the *ATH1* promoter and 5' untranslated region. Closed arrowhead mark the 5' end of genomic fragments used in construction of 2-kb and 3.3-kb *ATH1p:GUS* reporter genes. Predicted consensus binding sites for TGA bZIP factors (Schindler, 1992; Izawa et al., 1993; Fode et al., 2008) are shown in relation to fragments amplified by qRT-PCR after ChIP to test for BOP1 localization (horizontal bars). Sites in red (IV and VII) contain A-boxes and show enrichment for BOP1. J, Quantification of BOP1-GR enrichment at sites IV and VII in the *ATH1* promoter by qRT-PCR. Anti-GR ChIP was performed using leaves from Mock and DEX-treated *35S:BOP1-GR bop1 bop2* plants. Fold-enrichment at sites IV and VII is presented as the ratio of DEX versus Mock transcript levels after normalization to the unrelated UBQ5 control sequence. Three biological replicates were quantified to show enrichment at Site IV. One biological replicate was quantified to show enrichment at Site VII. Three technical replicates were performed for each. Error bars, s.d.

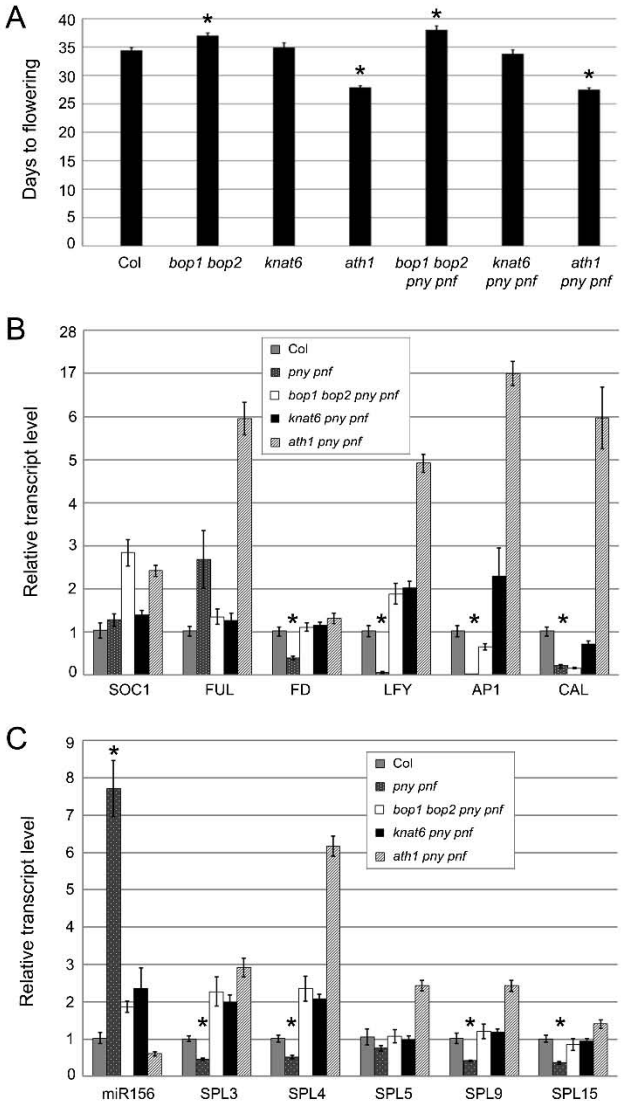

Figure 6. Quantification of flowering time and meristem-identity transcripts in wild-type and mutants. A, Quantitative analysis of flowering-time. Plants were grown under LDs. Date of apex emergence for *bop1 bop2 pny pnf*, *knat6 pny pnf*, and *ath1 pny pnf* mutants is comparable to wild-type with minor variations. Lines containing *ath1* flowered slightly earlier (-6.7 days) and lines containing *bop1 bop2* flowered slightly later (+3.1 days) than wild-type. Asterisks indicate significant differences (Student's *t* test, $p<0.01$). B, Quantitative analysis of meristem identity gene expression. Flowering was induced by shifting plants from SDs to LDs. Apices were harvested on Day 37 at the end of 12 LDs. Inflorescence meristem-identity gene transcripts *SOC1* and *FUL* are expressed at similar levels in Col and *pny pnf* apices. Floral meristem-identity gene transcripts *FD*, *LFY*, *AP1*, and *CAL* are significantly lower in *pny pnf* compared to Col apices. Transcript accumulation resumes in *bop1 bop2 pny pnf*, *knat6 pny pnf*, *ath1 pny pnf* apices. C, Quantitative analysis of *miR156* and *SPL* transcript abundance in wild-type and mutant apices. Non-flowering in *pny pnf* correlates with a significant increase in *miR156* abundance at the expense of *SPL3,4,6,9,* and *15* transcripts relative to Col plants. Transcript accumulation in *bop1 bop2 pny pnf*, *knat6 pny pnf*, *ath1 pny pnf* mutants follows a pattern similar to wild-type, consistent with restored flowering. Asterisks in B and C indicate significant differences (Student's *t* test, $p<0.05$).

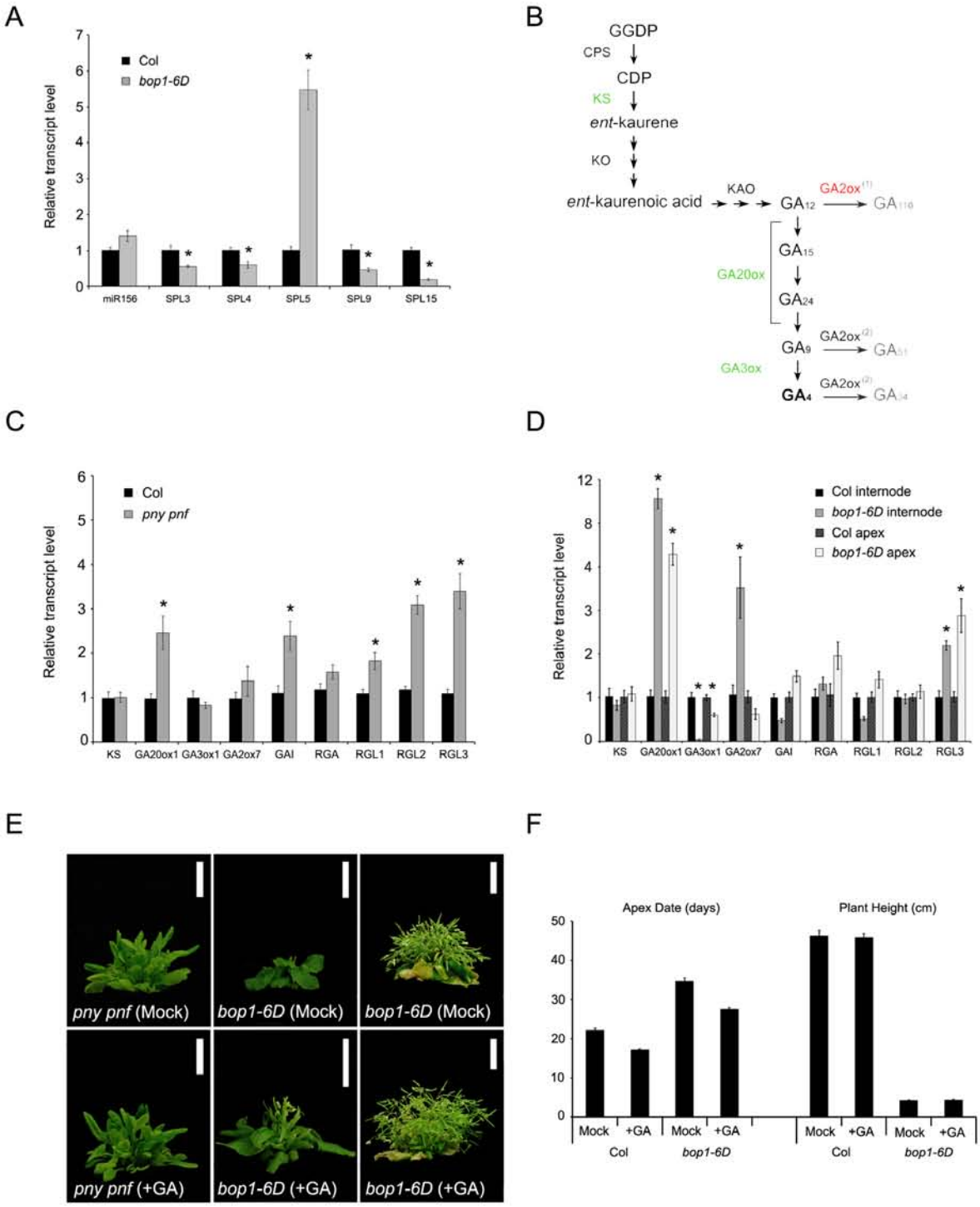

Figure 7. *BOP1* overexpression mimics *pny pnf* defects in *SPL* transcript accumulation and GA homeostasis. Plants were grown in continuous light. qRT-PCR was used to assess transcript accumulation in apices and/or internodes. A, Accumulation of *miR156* and *SPL* transcripts in Col and *bop1-6D* internodes. B, Schematic representation of non-13-hydroxylated GA biosynthetic and catabolic pathways in Arabidopsis (Hu et al., 2008; Yamaguchi, 2008). Green lettering, GA biosynthetic enzymes monitored for transcript accumulation in C, D. Red lettering, GA catabolic enzyme monitored for transcript accumulation in C, D. Bioactive GA4 in bold. Inactive GA metabolites shown on right. GGDP, geranylgeranyl diphosphate; CDP, ent-copalyl diphosphate; CPS, ent-copalyl diphosphate synthase; KS, ent-kaurene synthase; KO, ent-kaurene oxidase; KAO, ent-kaurenoic acid oxidase. C and D, Accumulation of GA pathway transcripts in *pny pnf* apices and *bop1-6D* apices and internodes. E, *pny pnf* and *bop1-6D* plants treated with 100 μm GA3 or a Mock solution. F, Flowering time and plant height of Col and *bop1-6D* plants treated with 100 μm GA3 or a Mock solution. Asterisks in A, C, and D indicate significant differences (Student's *t* test, $p < 0.05$).

A

Repressor	Gene Name	Log_2FC
DELLA		
At5g17490	*RGL3*	1.20
FLC-clade		
At1g77080	*MAF1 (AGL27)*	0.64
At5g65060	*MAF3 (AGL70)*	0.50
At5g65080	*MAF5 (AGL68)*	1.26
AP2-like		
At5g60120	*TOE2*	0.56
At3g54990	*SMZ*	0.80
AP2/ERF		
At1g12610	*DDF1*	3.22
At1g63030	*DDF2*	0.89
At4g25470	*CBF2*	1.25
At5g51990	*CBF4*	1.31
At1g12610	*TINY2*	0.55

B

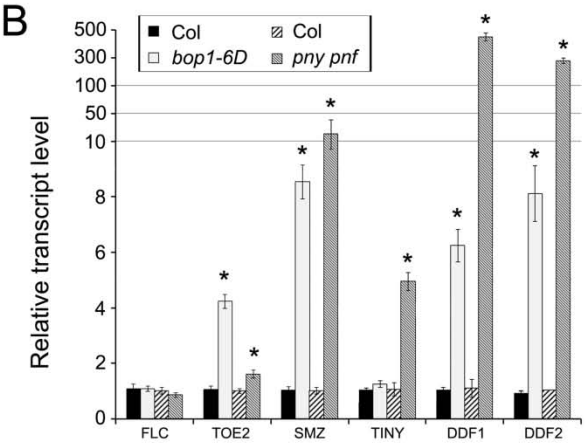

Figure 8. Transcript profiling of floral repressor genes in *bop1-6D* and *pny pnf* mutants. A, Floral repressor genes differentially expressed in *bop1-6D* compared to Col internodes according to microarray experiment (see Materials and Methods). B, Repressor transcript profile of *bop1-6D* and *pny pny* mutants quantified by qRT-PCR. No differential expression was observed for *FLC* transcript. Transcripts encoding AP2-like *TOE2* and *SMZ* repressors and AP2/ERF TINY, DDF1, and DDF2 repressors were differentially upregulated in agreement with (A). Asterisks indicate significant differences (Student's *t* test, $p<0.05$).

A

BIOSYNTHESIS	Gene Name	Log_2FC
At3g45140	*LOX2*	0.91
At1g72520	*LOX4*	0.85
At5g42650	*AOS*	1.13
At3g25770	*AOC2*	0.74
At3g25780	*AOC3*	1.39
At3g25780	*OPR3 (DDE1)*	1.03
SIGNALING		
At1g32640	*MYC2*	1.44

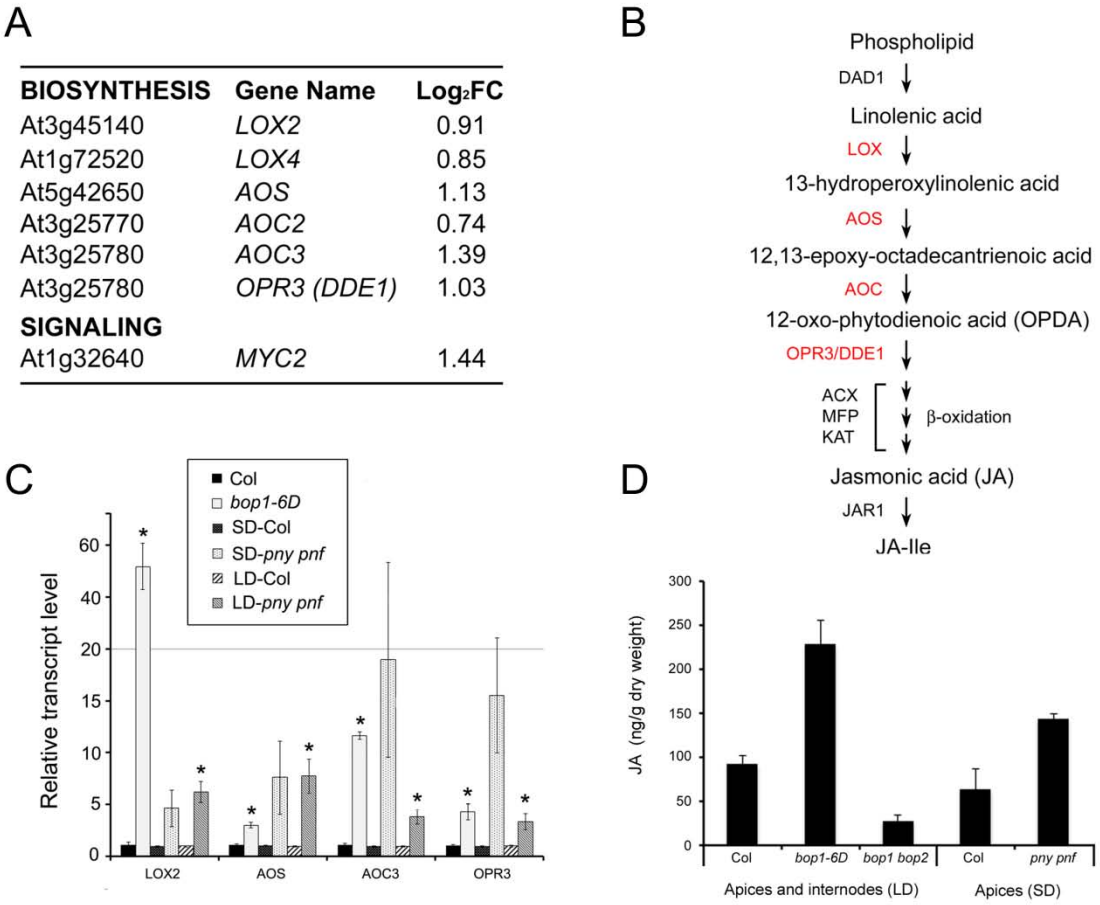

Figure 9. *BOP1* overexpression increases JA content by transcriptional upregulation of biosynthetic genes. A, JA-related genes differentially expressed in *bop1-6D* compared to Col internodes identified by microarray experiment (Materials and Methods). B, Schematic representation of JA biosynthetic pathway in Arabidopsis (Park et al., 2002; Wasternak and Hause, 2013). Red lettering, transcripts investigated by qRT-PCR in (C). Linolenic acid is released from membrane lipids by a lipolytic enzyme (DAD1/DEFECTIVE IN ANTHER DEHISCENCE1) and converted to allene oxide (12,13-epoxy-octadecantrienoic acid) by lipoxygenase (LOX) and allene oxide synthase (AOS). One cyclization, one reduction, and three rounds of β-oxidation steps are required in producing jasmonic acid (JA) which is conjugated to isoleucine (JA-Ile) in bioactive form (Wasternak and Kombrink, 2010). DAD1, DEFECTIVE IN ANTHER DEHISCENCE1; AOS, allene oxidase synthase; LOX, lipooxygenase; AOC, allene oxide cyclase; OPR3/DDE1, 12-oxo-phytodienoic acid-10,11-reductase3/DELAYED DEHISCENCE1; ACX, Acetyl-CoA oxidase; MPF, multifunctional protein; KAT, L-3-ketoacyl CoA thiolase; JAR1, JASMONATE RESISTANT1. C, Quantitative analysis of JA biosynthetic gene transcripts in *bop1-6D* and *pny pnf* mutants grown under SDs or LDs. Asterisks indicate significant differences (Student's *t* test, $p<0.05$). D, Concentration of JA in wild-type tissues compared to *bop1-6D*, *bop1 bop2*, and *pny pnf* mutants (see Materials and Methods).

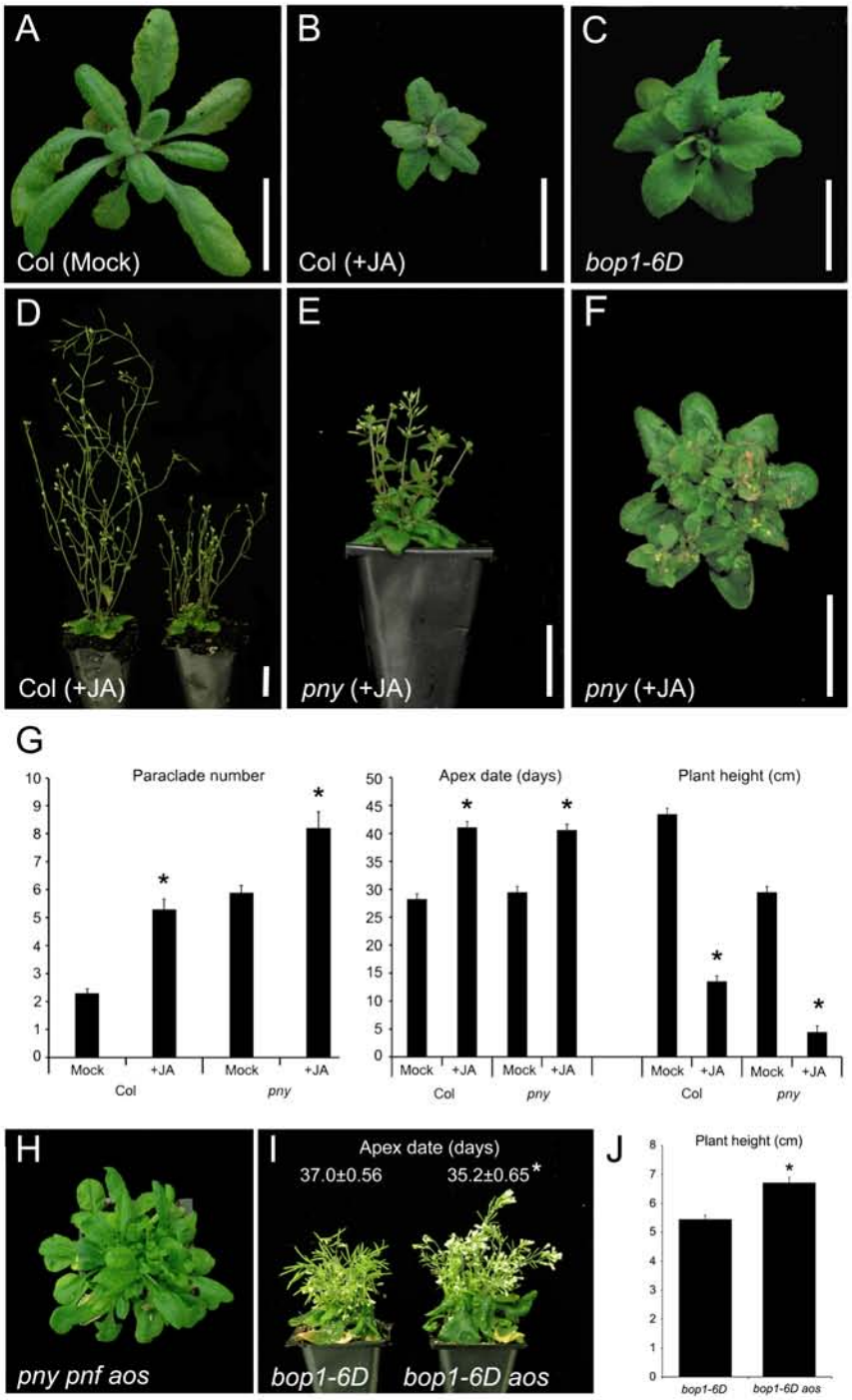

Figure 10. Effect of loss or gain of JA content on phenotype of wild-type and mutants. A-G, Wild-type and *pny* plants were sprayed daily until maturity with 100 µm MeJA or a Mock solution. A, Mock-treated Col plant. B, MeJA-treated Col plant showing small, dark green leaves. C, *bop1-6D* mutant showing a compact rosette similar to (B). D, JA-treated Col plants showing *pny*-like partial loss of apical dominance and short stature. E, JA-treated *pny* mutant showing enhancement of defects in internode elongation and apical dominance relative to Mock control (see G). F, JA-treated *pny* mutant showing delayed flowering relative to Mock control. G, Quantitative phenotypic analysis of wild-type and *pny* mutant plants treated with MeJA. Plants were grown under LDs. For both genotypes, treatment with MeJA resulted in additional rosette paraclades indicating loss of apical dominance, reduced height, and delayed flowering. Asterisks indicate significant differences (Student's t test, $p<0.05$). H-J, Effect of *aos* loss-of-function on *pny pnf* and *bop1-6D* phenotypes. Representative plants are shown. H, *pny pnf aos* mutant remains non-flowering. I-J, Phenotype of *bop1-6D* versus *bop1-6D aos* mutants. A small but highly significant ($p<0.0001$) increase in plant height (+1.26 cm) and earlier flowering (-1.8 days) is measured in *bop1-6D aos* compared to *bop1-6D* control plants.

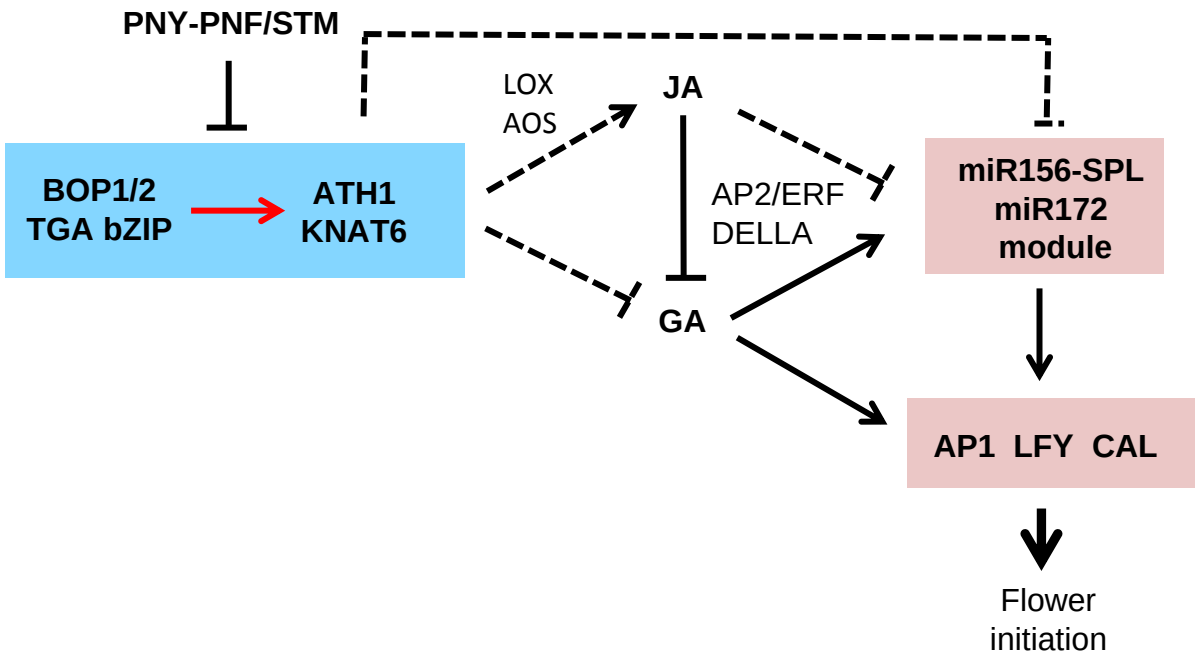

Figure 11. Summary and model. PNY-PNF/STM limit expression of *BOP1/2* and downstream effectors *ATH1/KNAT6* to boundary domains flanking the IM. BOP1 acting via an unknown TGA bZIP co-factor directly activates *ATH1* whereas promotion of *KNAT6* is indirect (red arrow). These products form a module that represses growth, meristem activity, and flowering by increasing JA content via transcriptional promotion of JA biosynthetic genes. Either directly or indirectly (dashed lines), we propose that misexpression of this pathway leads to down-regulation of GA pathway components and repression of the *miR156-SPL-miR172* module at one or more nodes in correlation with increased content of associated classes of floral repressors (e.g. DELLA, AP2-like, and AP2/ERF clades). Ultimately, *SPL* and *FD/FT* transcripts (not depicted) fail to accumulate and activation of floral meristem identity genes *LFY*, *AP1*, and *CAL* required for flower initiation is blocked. Internode elongation is also blocked.

Parsed Citations

Abe M, Kobayashi Y, Yamamoto S, Daimon Y, Yamaguchi A, Ikeda Y, Ichinoki H, Notaguchi M, Goto K, Araki T (2005) FD, a bZIP protein mediating signals from the floral pathway integrator FT at the shoot apex. Science 309: 1052-1056
Pubmed: Author and Title
CrossRef: Author and Title
Google Scholar: Author Only Title Only Author and Title

Aichinger E, Kornet N, Friedrich T, Laux T (2012) Plant stem cell niches. Annu Rev Plant Biol 63: 615-636
Pubmed: Author and Title
CrossRef: Author and Title
Google Scholar: Author Only Title Only Author and Title

Aida M, Tasaka M (2006) Genetic control of shoot organ boundaries. Curr Opin Plant Biol 9: 72-77
Pubmed: Author and Title
CrossRef: Author and Title
Google Scholar: Author Only Title Only Author and Title

Albrechtová J, Ullmann J (1994) Methyl jasmonate inhibits growth and flowering in Chenopodium rubrum. Biol Plantarum 36: 317-319
Pubmed: Author and Title
CrossRef: Author and Title
Google Scholar: Author Only Title Only Author and Title

Amasino RM, Michaels SD (2010) The timing of flowering. Plant Physiol 154: 516-520
Pubmed: Author and Title
CrossRef: Author and Title
Google Scholar: Author Only Title Only Author and Title

Andrés F, Coupland G (2012) The genetic basis of flowering responses to seasonal cues. Nat Rev Genet 13: 627-639
Pubmed: Author and Title
CrossRef: Author and Title
Google Scholar: Author Only Title Only Author and Title

Andre´s F, Romera-Branchat M, Marti´nez-Gallegos R, Patel V, Schneeberger K, Jang S, Altmu¨ller J, Nu¨rnberg P, Coupland G (2015) Floral induction in Arabidopsis thaliana by FLOWERING LOCUS T requires direct repression of BLADE-ON-PETIOLE genes by homeobox protein PENNYWISE. Plant Physiol, this issue
Pubmed: Author and Title
CrossRef: Author and Title
Google Scholar: Author Only Title Only Author and Title

Aukerman M, Sakai H (2003) Regulation of flowering time and floral organ identity by a microRNA and its APETALA2-like target genes. Plant Cell 15: 2730-2741
Pubmed: Author and Title
CrossRef: Author and Title
Google Scholar: Author Only Title Only Author and Title

Belles-Boix E, Hamant O, Witiak SM, Morin H, Traas J, Pautot V (2006) KNAT6: an Arabidopsis homeobox gene involved in meristem activity and organ separation. Plant Cell 18: 1900-1907
Pubmed: Author and Title
CrossRef: Author and Title
Google Scholar: Author Only Title Only Author and Title

Bernier G (1988) The control of floral evocation and morphogenesis. Annu Rev Plant Physiol 39: 175-219
Pubmed: Author and Title
CrossRef: Author and Title
Google Scholar: Author Only Title Only Author and Title

Bonaventure G, Gfeller A, Proebsting WM, Hörsteiner S, Chételat A, Martinoia E, Farmer EE (2007) A gain-of-function allele of TPC1 activates oxylipin biogenesis after leaf wounding in Arabidopsis. Plant J 49: 899-898
Pubmed: Author and Title
CrossRef: Author and Title
Google Scholar: Author Only Title Only Author and Title

Bowman J, Alvarez J, Weigel D, Meyerowitz E (1993) Control of flower development in Arabidopsis thaliana by APETALA1 and interacting genes. Development 119: 721-743
Pubmed: Author and Title
CrossRef: Author and Title
Google Scholar: Author Only Title Only Author and Title

Boyle P, Le Su E, Rochon A, Shearer HL, Murmu J, Chu JY, Fobert PR, Després C (2009) The BTB/POZ domain of the Arabidopsis disease resistance protein NPR1 interacts with the repression domain of TGA2 to negate its function. Plant Cell 21: 3700-3713
Pubmed: Author and Title
CrossRef: Author and Title
Google Scholar: Author Only Title Only Author and Title

Byrne ME, Barley R, Curtis M, Arroyo JM, Dunham M, Hudson A, Martienssen RA (2000) Asymmetric leaves1 mediates leaf patterning and stem cell function in Arabidopsis. Nature 408: 967-971
Pubmed: Author and Title
CrossRef: Author and Title

Google Scholar: Author Only Title Only Author and Title

Byrne ME, Groover AT, Fontana JR, Martienssen RA (2003) Phyllotactic pattern and stem cell fate are determined by the Arabidopsis homeobox gene BELLRINGER. Development 130: 3941-3950
Pubmed: Author and Title
CrossRef: Author and Title
Google Scholar: Author Only Title Only Author and Title

Canet J, Dobón A, Fajmonová J, Tornero P (2012) The BLADE-ON-PETIOLE genes of Arabidopsis are essential for resistance induced by methyl jasmonate. BMC Plant Biol 12: 199
Pubmed: Author and Title
CrossRef: Author and Title
Google Scholar: Author Only Title Only Author and Title

Chakravarthy S, Tuori RP, D'Ascenzo MD, Fobert PR, Després C, Martin GB (2003) The tomato transcription factor Pti4 regulates defense-related gene expression via GCC box and non-GCC box cis elements. Plant Cell 15: 3033-3050
Pubmed: Author and Title
CrossRef: Author and Title
Google Scholar: Author Only Title Only Author and Title

Cho S, Coruh C, Axtell M (2012) miR156 and miR360 regulate tasiRNA accumulation and developmental timing in Physcomitrella patens. Plant Cell 24: 4837-4849
Pubmed: Author and Title
CrossRef: Author and Title
Google Scholar: Author Only Title Only Author and Title

Cipollini D (2005) Interactive effects of lateral shading and jasmonic acid on morphology, phenology, seed production,and defense traits in Arabidopsis thaliana. Int J Plant Sci 166: 955-959
Pubmed: Author and Title
CrossRef: Author and Title
Google Scholar: Author Only Title Only Author and Title

Clark SE, Jacobsen SE, Levin JZ, Meyerowitz EM (1996) The CLAVATA and SHOOT MERISTEMLESS loci competitively regulate meristem activity in Arabidopsis. Development 122: 1567-1575
Pubmed: Author and Title
CrossRef: Author and Title
Google Scholar: Author Only Title Only Author and Title

Clough SJ, Bent AF (1998) Floral dip: a simplified method for Agrobacterium-mediated transformation of Arabidopsis thaliana. Plant J 16: 735-743
Pubmed: Author and Title
CrossRef: Author and Title
Google Scholar: Author Only Title Only Author and Title

Corbesier L, Vincent C, Jang S, Fornara F, Fan Q, Searle I, Giakountis A, Farrona S, Gissot L, Turnbull C, Coupland G (2007) FT protein movement contributes to long-distance signaling in floral induction of Arabidopsis. Science 316: 1030-1033
Pubmed: Author and Title
CrossRef: Author and Title
Google Scholar: Author Only Title Only Author and Title

Cui L-G, Shan J-X, Shi M, Gao J-P, Lin H-X (2014) The miR156-SPL9-DFR pathway coordinates the relationship between development and abiotic stress tolerance in plants. Plant J 80: 1108-1117
Pubmed: Author and Title
CrossRef: Author and Title
Google Scholar: Author Only Title Only Author and Title

Després C, DeLong C, Glaze S, Liu E, Fobert PR (2000) The Arabidopsis NPR1/NIM1 protein enhances the DNA binding activity of a subgroup of the TGA family of bZIP transcription factors. Plant Cell 12: 279-290
Pubmed: Author and Title
CrossRef: Author and Title
Google Scholar: Author Only Title Only Author and Title

Diallo A, Agharbaoui Z, Badawi M, Ali-Benali M, Moheb A, Houde M, Sarhan F (2014) Transcriptome analysis of an mvp mutant reveals important changes in global gene expression and a role for methyl jasmonate in vernalization and flowering in wheat. J Exp Bot 65: 2271-2286
Pubmed: Author and Title
CrossRef: Author and Title
Google Scholar: Author Only Title Only Author and Title

Dill A, Thomas S, Hu J, Steber C, Sun T-P (2004) The Arabidopsis F-box protein SLEEPY1 targets gibberellin signaling repressors for gibberellin-induced degradation. Plant Cell 16: 1392-1405
Pubmed: Author and Title
CrossRef: Author and Title
Google Scholar: Author Only Title Only Author and Title

Ellis C, I. K, Wasternak C, Turner JG (2002) The Arabidopsis mutant cev1 links cell wall signaling to jasmonate and ethylene responses. Plant Cell 14: 1557-1566
Pubmed: Author and Title
CrossRef: Author and Title
Google Scholar: Author Only Title Only Author and Title

Endrizzi K, Moussian B, Haecker A, Levin JZ, Laux T (1996) The SHOOT MERISTEMLESS gene is required for maintenance of undifferentiated cells in Arabidopsis shoot and floral meristems and acts at a different regulatory level than the meristem genes WUSCHEL and ZWILLE. Plant J 10: 967-979
Pubmed: Author and Title
CrossRef: Author and Title
Google Scholar: Author Only Title Only Author and Title

Eriksson S, Bohlenius H, Moritz T, Nilsson O (2006) GA4 is the active gibberellin in the regulation of LEAFY transcription and Arabidopsis floral initiation. Plant Cell 18: 2171-2181
Pubmed: Author and Title
CrossRef: Author and Title
Google Scholar: Author Only Title Only Author and Title

Etchells J, Moore L, Jiang WZ, Prescott H, Capper R, Saunders NJ, Bhatt AM, Dickinson HG (2012) A role for BELLRINGER in cell wall development is supported by loss-of-function phenotypes. BMC Plant Biol 12: 212
Pubmed: Author and Title
CrossRef: Author and Title
Google Scholar: Author Only Title Only Author and Title

Fode B, Siemsen T, Thurow C, R W, Gatz C (2008) The Arabidopsis GRAS protein SCL14 interacts with class II TGA transcription factors and is essential for the activation of stress-inducible promoters. Plant Cell 20: 3122-3135
Pubmed: Author and Title
CrossRef: Author and Title
Google Scholar: Author Only Title Only Author and Title

Galvão V, Horrer D, Küttner F, Schmid M (2012) Spatial control of flowering by DELLA proteins in Arabidopsis thaliana. Development 139: 4072-4082
Pubmed: Author and Title
CrossRef: Author and Title
Google Scholar: Author Only Title Only Author and Title

Gentleman RC, Carey VJ, Bates DM, Bolstad B, Dettling M, Dudoit S, Ellis B, Gautier L, Ge Y, Gentry J, Hornik K, Hothorn T, Huber W, Iacus S, Irizarry R, Leisch F, Li C, Maechler M, Rossini AJ, Sawitzki G, Smith C, Smyth G, Tierney L, Yang JY, Zhang J (2004) Bioconductor: open software development for computational biology and bioinformatics. Genome Biol 5: R80
Pubmed: Author and Title
CrossRef: Author and Title
Google Scholar: Author Only Title Only Author and Title

Gómez-Mena C, Sablowski R (2008) ARABIDOPSIS THALIANA HOMEOBOX GENE1 establishes the basal boundaries of shoot organs and controls stem growth. Plant Cell 20: 2059-2072
Pubmed: Author and Title
CrossRef: Author and Title
Google Scholar: Author Only Title Only Author and Title

Ha CM, Jun JH, Nam HG, Fletcher JC (2007) BLADE-ON-PETIOLE 1 and 2 control Arabidopsis lateral organ fate through regulation of LOB domain and adaxial-abaxial polarity genes. Plant Cell 19: 1809-1825
Pubmed: Author and Title
CrossRef: Author and Title
Google Scholar: Author Only Title Only Author and Title

Hamama L, Naouar A, Gala R, Voisine L, Pierre S, Jeauffre J, Cesbron D, Leplat F, Foucher F, Dorion N, Hibrand-Saint Oyant L (2012) Overexpression of the RoDELLA impacts the height, branching, and flowering behaviour of Pelargonium X domesticum transgenic plants. Plant Cell Rep 31: 2015-2029
Pubmed: Author and Title
CrossRef: Author and Title
Google Scholar: Author Only Title Only Author and Title

Hamant O, Pautot V (2010) Plant development: a TALE story. CR Biol 333: 371-381
Pubmed: Author and Title
CrossRef: Author and Title
Google Scholar: Author Only Title Only Author and Title

Haughn GW, Somerville C (1986) Sulfonylurea-resistant mutants of Arabidopsis thaliana. Mol Gen Genet 204: 430-434
Pubmed: Author and Title
CrossRef: Author and Title
Google Scholar: Author Only Title Only Author and Title

Hay A, Kaur H, Phillips A, Hedden P, Hake S, Tsiantis M (2002) The gibberellin pathway mediates KNOTTED1-type homeobox function in plants with different body plans. Curr Biol 12: 1557-1565
Pubmed: Author and Title
CrossRef: Author and Title
Google Scholar: Author Only Title Only Author and Title

Hay A, Tsiantis M (2010) KNOX genes: versatile regulators of plant development and diversity. Development 137: 3153-3165
Pubmed: Author and Title
CrossRef: Author and Title
Google Scholar: Author Only Title Only Author and Title

Heckman KL, Pease LR (2007) Gene splicing and mutagenesis by PCR-driven overlap extension. Nat Protoc 2: 924-932
Pubmed: Author and Title

CrossRef: Author and Title
Google Scholar: Author Only Title Only Author and Title

Heinrich M, Hettenhausen C, Lange T, Wunsche H, Fang J, Baldwin I, Wu J (2013) High levels of jasmonic acid antagonize the biosynthesis of gibberellins and inhibit the growth of Nicotiana attenuata stems. Plant J 73: 591-606
Pubmed: Author and Title
CrossRef: Author and Title
Google Scholar: Author Only Title Only Author and Title

Hellens RP, Edwards EA, Leyland NR, Bean S, Mullineaux PM (2000) pGreen: a versatile and flexible binary Ti vector for Agrobacterium-mediated plant transformation. Plant Mol Biol 42: 819-832
Pubmed: Author and Title
CrossRef: Author and Title
Google Scholar: Author Only Title Only Author and Title

Hepworth SR, Valverde F, Ravenscroft D, Mouradov A, Coupland G (2002) Antagonistic regulation of flowering-time gene SOC1 by CONSTANS and FLC via separate promoter motifs. EMBO J 21: 4327-4337
Pubmed: Author and Title
CrossRef: Author and Title
Google Scholar: Author Only Title Only Author and Title

Hepworth SR, Zhang Y, McKim S, Li X, Haughn GW (2005) BLADE-ON-PETIOLE-dependent signaling controls leaf and floral patterning in Arabidopsis. Plant Cell 17: 1434-1448
Pubmed: Author and Title
CrossRef: Author and Title
Google Scholar: Author Only Title Only Author and Title

Hou X, Ding L, Yu H (2013) Crosstalk between GA and JA signaling mediates plant growth and defense. Plant Cell Rep 32: 1067-1074
Pubmed: Author and Title
CrossRef: Author and Title
Google Scholar: Author Only Title Only Author and Title

Hu J, Mitchum M, Barnaby N, Ayele B, Ogawa M, Nam E, Lai W-C, Hanada A, Alonso J, Ecker J, Swain S, Yamaguchi S, Kamiya Y, Sun T-P (2008) Potential sites of bioactive gibberellin production during reproductive growth in Arabidopsis. Plant Cell 20: 320-336
Pubmed: Author and Title
CrossRef: Author and Title
Google Scholar: Author Only Title Only Author and Title

Huijser P, Schmid M (2011) The control of developmental phase transitions in plants. Development 138: 4117-4129
Pubmed: Author and Title
CrossRef: Author and Title
Google Scholar: Author Only Title Only Author and Title

Hyun Y, Choi S, Hwang H-J, Yu J, Nam S-J, Ko J, Park J-Y, Seo YS, Kim EY, Ryu SB, Kim WT, Lee YH, Kang H, Lee I (2008) Cooperation and functional diversification of two closely related galactolipase genes for jasmonate biosynthesis. Dev Cell 14: 183-192
Pubmed: Author and Title
CrossRef: Author and Title
Google Scholar: Author Only Title Only Author and Title

Izawa T, Foster R, Chua N-H (1993) Plant bZIP protein DNA binding specificity. J Mol Biol 230: 1131-1144
Pubmed: Author and Title
CrossRef: Author and Title
Google Scholar: Author Only Title Only Author and Title

Jaeger KE, Wigge PA (2007) FT protein acts as a long-range signal in Arabidopsis. Curr Biol 17: 1050-1054
Pubmed: Author and Title
CrossRef: Author and Title
Google Scholar: Author Only Title Only Author and Title

Jun JH, Ha CM, Fletcher JC (2010) BLADE-ON-PETIOLE1 coordinates organ determinacy and axial polarity in arabidopsis by directly activating ASYMMETRIC LEAVES2. Plant Cell 22: 62-76
Pubmed: Author and Title
CrossRef: Author and Title
Google Scholar: Author Only Title Only Author and Title

Jung J-H, Seo Y-H, Seo P, Reyes J, Yun J, Chua N-H, Park C-M (2007) The GIGANTEA-regulated miRNA172 mediates photoperiodic flowering independent of CONSTANS in Arabidopsis. Plant Cell 19: 2736-2748
Pubmed: Author and Title
CrossRef: Author and Title
Google Scholar: Author Only Title Only Author and Title

Jung JH, Ju Y, Seo PJ, Lee JH, Park CM (2012) The SOC1-SPL module integrates photoperiod and gibberellic acid signals to control flowering time in Arabidopsis. Plant J 69: 577-588
Pubmed: Author and Title
CrossRef: Author and Title
Google Scholar: Author Only Title Only Author and Title

Kang H-G, Kim J, Kim B, Jeong H, Choi SH, Kim EK, Lee H-Y, Lim PO (2011) Overexpression of FTL1/DDF1, an AP2 transcription factor, enhances tolerance to cold, drought, and heat stresses in Arabidopsis thaliana. Plant Sci 180: 634-641

Pubmed: Author and Title
CrossRef: Author and Title
Google Scholar: Author Only Title Only Author and Title

Kanrar S, Bhattacharya M, Arthur B, Courtier J, Smith HMS (2008) Regulatory networks that function to specify flower meristems require the function of homeobox genes PENNYWISE and POUND-FOOLISH in Arabidopsis. Plant J 54: 924-937
Pubmed: Author and Title
CrossRef: Author and Title
Google Scholar: Author Only Title Only Author and Title

Kanrar S, Onguka O, Smith HMS (2006) Arabidopsis inflorescence architecture requires the activities of KNOX-BELL homeodomain heterodimers. Planta 224: 1163-1173
Pubmed: Author and Title
CrossRef: Author and Title
Google Scholar: Author Only Title Only Author and Title

Kardailsky I, Shukla VK, Ahn JH, Dagenais N, Christensen SK, Nguyen JT, Chory J, Harrison MJ, Weigel D (1999) Activation tagging of the floral inducer FT. Science 286: 1962-1965
Pubmed: Author and Title
CrossRef: Author and Title
Google Scholar: Author Only Title Only Author and Title

Khan M, Tabb P, Hepworth SR (2012a) BLADE-ON-PETIOLE1 and 2 regulate Arabidopsis inflorescence architecture in conjunction with homeobox genes KNAT6 and ATH1. Plant Signal Behav 7: 788-792
Pubmed: Author and Title
CrossRef: Author and Title
Google Scholar: Author Only Title Only Author and Title

Khan M, Xu H, Hepworth SR (2014) BLADE-ON-PETIOLE genes: setting boundaries in development and defense. Plant Sci 215-216: 157-171
Pubmed: Author and Title
CrossRef: Author and Title
Google Scholar: Author Only Title Only Author and Title

Khan M, Xu M, Murmu J, Tabb P, Liu Y, Storey K, McKim SM, Douglas CJ, Hepworth SR (2012b) Antagonistic interaction of BLADE-ON-PETIOLE1 and 2 with BREVIPEDICELLUS and PENNYWISE regulates Arabidopsis inflorescence architecture. Plant Physiol 158: 946-960
Pubmed: Author and Title
CrossRef: Author and Title
Google Scholar: Author Only Title Only Author and Title

Kim J, Lee JH, Kim W, Jung HS, Huijser P, Ahn JH (2012) The microRNA156-SQUAMOSA PROMOTER BINDING PROTEIN-LIKE3 module regulates ambient temperature-responsive flowering via FLOWERING LOCUS T in Arabidopsis. Plant Physiol 159: 461-478
Pubmed: Author and Title
CrossRef: Author and Title
Google Scholar: Author Only Title Only Author and Title

Koncz C, Schell J (1986) The promoter of TL-DNA gene 5 controls the tissue-specific expression of chimeric genes carried by a novel type of Agrobacterium binary vector. Mol Gen Genet 204: 383-396
Pubmed: Author and Title
CrossRef: Author and Title
Google Scholar: Author Only Title Only Author and Title

Lal S, Pacis LB, Smith HM (2011) Regulation of the SQUAMOSA PROMOTER-BINDING PROTEIN-LIKE genes/microRNA156 module by the homeodomain proteins PENNYWISE and POUND-FOOLISH in Arabidopsis. Mol Plant 4: 1123-1132
Pubmed: Author and Title
CrossRef: Author and Title
Google Scholar: Author Only Title Only Author and Title

Le Roux C, Del Prete S, Boutet-Mercey S, Perreau F, Balagué C, Roby D, Fagard M, Gaudin V (2014) The hnRNP-Q protein LIF2 participates in the plant immune response. PLoS One 9: e99343
Pubmed: Author and Title
CrossRef: Author and Title
Google Scholar: Author Only Title Only Author and Title

Li Y, Pi L, Huang H, Xu L (2012) ATH1 and KNAT2 proteins act together in regulation of plant inflorescence architecture. J Exp Bot 63: 1423-1433
Pubmed: Author and Title
CrossRef: Author and Title
Google Scholar: Author Only Title Only Author and Title

Licausi F, Ohme-Takagi M, Perata P (2013) APETALA2/Ethylene Responsive Factor (AP2/ERF) transcription factors: mediators of stress responses and developmental programs. New Phytol 199: 639-649
Pubmed: Author and Title
CrossRef: Author and Title
Google Scholar: Author Only Title Only Author and Title

Lincoln C, Long J, Yamaguchi J, Serikawa K, Hake S (1994) A knotted1-like homeobox gene in Arabidopsis is expressed in the vegetative meristem and dramatically alters leaf morphology when overexpressed in transgenic plants. Plant Cell 6: 1859-1876
Pubmed: Author and Title
CrossRef: Author and Title

Google Scholar: Author Only Title Only Author and Title

Lloyd AM, Schena M, Walbot V, Davis RW (1994) Epidermal cell fate determination in Arabidopsis: patterns defined by a steroid-inducible regulator. Science 266: 436-439
Pubmed: Author and Title
CrossRef: Author and Title
Google Scholar: Author Only Title Only Author and Title

Long JA, Moan EI, Medford JI, Barton MK (1996) A member of the KNOTTED class of homeodomain proteins encoded by the STM gene of Arabidopsis. Nature 379: 66-69
Pubmed: Author and Title
CrossRef: Author and Title
Google Scholar: Author Only Title Only Author and Title

Maciejewska B, Kopceiwicz J (2002) Inhibitory effect of methyl jasmonate on flowering and elongation growth in Pharbitis nil. J Plant Growth Regul 21: 216-223
Pubmed: Author and Title
CrossRef: Author and Title
Google Scholar: Author Only Title Only Author and Title

Maciejewska BD, Kesy J, Zielinska M, Kopcewicz J (2004) Jasmonates inhibit flowering in short-day plant Pharbitis nil. Plant Growth Regul 43: 1-8
Pubmed: Author and Title
CrossRef: Author and Title
Google Scholar: Author Only Title Only Author and Title

Magome H, Yamaguchi S, Hanada A, Kamiya Y, Oda K (2008) The DDF1 transcriptional activator upregulates expression of a gibberellin-deactivating gene, GA2ox7, under high-salinity stress in Arabidopsis. Plant J 56: 613-626
Pubmed: Author and Title
CrossRef: Author and Title
Google Scholar: Author Only Title Only Author and Title

Magome H, Yamguchi S, Hanada A, Kamiya Y, Oda K (2004) Dwarf and delayed-flowering 1, a novel Arabidopsis mutant deficient in gibberellin biosynthesis because of overexpression of a putative AP2 transcription factor. Plant J 37: 720-729
Pubmed: Author and Title
CrossRef: Author and Title
Google Scholar: Author Only Title Only Author and Title

Mathieu J, Warthmann N, Kuttner F, Schmid M (2007) Export of FT protein from phloem companion cells is sufficient for floral induction in Arabidopsis. Curr Biol 17: 1055-1060
Pubmed: Author and Title
CrossRef: Author and Title
Google Scholar: Author Only Title Only Author and Title

Mathieu J, Yant LJ, Murdter F, Kuttner F, Schmid M (2009) Repression of flowering by the miR172 target SMZ. PLoS Biol 7: e1000148
Pubmed: Author and Title
CrossRef: Author and Title
Google Scholar: Author Only Title Only Author and Title

Matsoukas I, Massiah AJ, Thomas B (2012) Florigenic and antiflorigenic signaling in plants. Plant Cell Physiol 53: 1827-1842
Pubmed: Author and Title
CrossRef: Author and Title
Google Scholar: Author Only Title Only Author and Title

McKim SM, Stenvik GE, Butenko MA, Kristiansen W, Cho SK, Hepworth SR, Aalen RB, Haughn GW (2008) The BLADE-ON-PETIOLE genes are essential for abscission zone formation in Arabidopsis. Development 135: 1537-1546
Pubmed: Author and Title
CrossRef: Author and Title
Google Scholar: Author Only Title Only Author and Title

Mele G, Ori N, Sato Y, Hake S (2003) The knotted1-like homeobox gene BREVIPEDICELLUS regulates cell differentiation by modulating metabolic pathways. Genes Dev 17: 2088-2093
Pubmed: Author and Title
CrossRef: Author and Title
Google Scholar: Author Only Title Only Author and Title

Mutasa-Göttgens E, Hedden P (2009) Gibberellin as a factor in floral regulatory networks. J Exp Bot 60: 1979-1989
Pubmed: Author and Title
CrossRef: Author and Title
Google Scholar: Author Only Title Only Author and Title

Nakamichi N, Kiba T, Henriques R, Mizuno T, Chua NH, Sakakibara H (2010) PSEUDO-RESPONSE REGULATORS 9, 7, and 5 are transcriptional repressors in the Arabidopsis circadian clock. Plant Cell 22: 594-605
Pubmed: Author and Title
CrossRef: Author and Title
Google Scholar: Author Only Title Only Author and Title

Navarro L, Bari R, Achard P, Lison P, Nemri A, Harberd NP, Jones JDG (2008) DELLAs control plant immune responses by modulating the balance of jasmonic acid and salicylic acid signaling. Curr. Biol. 16: 650-655
Pubmed: Author and Title

CrossRef: Author and Title
Google Scholar: Author Only Title Only Author and Title

Nikovics K, Blein T, Peaucelle A, Ishida T, Morin H, Aida M, Laufs P (2006) The balance between the MIR164A and CUC2 genes controls leaf margin serration in Arabidopsis. Plant Cell 18: 2929-2945
Pubmed: Author and Title
CrossRef: Author and Title
Google Scholar: Author Only Title Only Author and Title

Norberg M, Holmlund M, Nilsson O (2005) The BLADE ON PETIOLE genes act redundantly to control the growth and development of lateral organs. Development 132: 2203-2213
Pubmed: Author and Title
CrossRef: Author and Title
Google Scholar: Author Only Title Only Author and Title

Park J-H, Halitschke R, Kim BH, Baldwin IT, Feldmann K, Feyereisen R (2002) A knock-out mutation in allene oxide synthase results in male sterility and defective wound signal transduction in Arabidopsis due to a block in jasmonic acid biosynthesis. Plant J 31: 1-12
Pubmed: Author and Title
CrossRef: Author and Title
Google Scholar: Author Only Title Only Author and Title

Peaucelle A, Louvet R, Johansen JN, Salsac F, Morin H, Fournet F, Belcram K, Gillet F, Höfte H, Laufs P, Mouille G, Pelloux J (2011) The transcription factor BELLRINGER modulates phyllotaxis by regulating the expression of a pectin methylesterase in Arabidopsis. Development 138: 4733-4741
Pubmed: Author and Title
CrossRef: Author and Title
Google Scholar: Author Only Title Only Author and Title

Porri A, Torti S, Romera-Branchat M, Coupland G (2012) Spatially distinct regulatory roles for gibberellins in the promotion of flowering of Arabidopsis under long photoperiods. Development 139: 2198-2209
Pubmed: Author and Title
CrossRef: Author and Title
Google Scholar: Author Only Title Only Author and Title

Proveniers M (2013) Sugars speed up the circle of life. eLife 2: e00625
Pubmed: Author and Title
CrossRef: Author and Title
Google Scholar: Author Only Title Only Author and Title

Proveniers M, Rutjens B, Brand M, Smeekens S (2007) The Arabidopsis TALE homeobox gene ATH1 controls floral competency through positive regulation of FLC. Plant J 52: 899-913
Pubmed: Author and Title
CrossRef: Author and Title
Google Scholar: Author Only Title Only Author and Title

Ragni L, Belles-Boix E, Gunl M, Pautot V (2008) Interaction of KNAT6 and KNAT2 with BREVIPEDICELLUS and PENNYWISE in Arabidopsis inflorescences. Plant Cell 20: 888-900
Pubmed: Author and Title
CrossRef: Author and Title
Google Scholar: Author Only Title Only Author and Title

Rutjens B, Bao D, van Eck-Stouten E, Brand M, Smeekens S, Proveniers M (2009) Shoot apical meristem function in Arabidopsis requires the combined activities of three BEL1-like homeodomain proteins. Plant J 58: 641-654
Pubmed: Author and Title
CrossRef: Author and Title
Google Scholar: Author Only Title Only Author and Title

Schindler U, Beckman, H., and Cashmore, A.R. (1992) TGA1 and G-box binding factors: two distinct classes of Arabidopsis leucine zipper proteins compete for the G-box-like element TGACGTGG. Plant Cell 4: 1309-1319
Pubmed: Author and Title
CrossRef: Author and Title
Google Scholar: Author Only Title Only Author and Title

Shi CL, Stenvik GE, Vie AK, Bones AM, Pautot V, Proveniers M, Aalen RB, Butenko MA (2011) Arabidopsis class I KNOTTED-like homeobox proteins act downstream in the IDA-HAE/HSL2 floral abscission signaling pathway. Plant Cell 23: 2553-2567
Pubmed: Author and Title
CrossRef: Author and Title
Google Scholar: Author Only Title Only Author and Title

Sieburth LE, Meyerowitz EM (1997) Molecular dissection of the AGAMOUS control region shows that cis elements for spatial regulation are located intragenically. Plant Cell 9: 355-365
Pubmed: Author and Title
CrossRef: Author and Title
Google Scholar: Author Only Title Only Author and Title

Smith HM, Campbell BC, Hake S (2004) Competence to respond to floral inductive signals requires the homeobox genes PENNYWISE and POUND-FOOLISH. Curr Biol 14: 812-817
Pubmed: Author and Title
CrossRef: Author and Title
Google Scholar: Author Only Title Only Author and Title

Smith HM, Hake S (2003) The interaction of two homeobox genes, BREVIPEDICELLUS and PENNYWISE, regulates internode patterning in the Arabidopsis inflorescence. Plant Cell 15: 1717-1727
Pubmed: Author and Title
CrossRef: Author and Title
Google Scholar: Author Only Title Only Author and Title

Smith HM, Ung N, Lal S, Courtier J (2011) Specification of reproductive meristems requires the combined function of SHOOT MERISTEMLESS and floral integrators FLOWERING LOCUS T and FD during Arabidopsis inflorescence development. J Exp Bot 62: 583-593
Pubmed: Author and Title
CrossRef: Author and Title
Google Scholar: Author Only Title Only Author and Title

Smyth DR, Bowman JL, Meyerowitz EM (1990) Early flowering development in Arabidopsis. Plant Cell 2: 755-767
Pubmed: Author and Title
CrossRef: Author and Title
Google Scholar: Author Only Title Only Author and Title

Smyth GK (2005) Limma: linear models for microarray data. In RC Gentleman, VJ Carey, S Dudoit, R Irizarry, W Huber, eds, Bioinformatics and computational biology solutions using R and Bioconductor. Springer, New York, pp 397-420
Pubmed: Author and Title
CrossRef: Author and Title
Google Scholar: Author Only Title Only Author and Title

Srikanth A, Schmid M (2011) Regulation of flowering time: all roads lead to Rome. Cell Mol Life Sci 68: 2013-2037
Pubmed: Author and Title
CrossRef: Author and Title
Google Scholar: Author Only Title Only Author and Title

Stief A, Altmann S, Hoffmann K, Pant BD, Scheible W-R, Bäurle I (2014) Arabidopsis miR156 regulates tolerance to recurring environmental stress through SPL transcription factors. Plant Cell 26: 1792-1807
Pubmed: Author and Title
CrossRef: Author and Title
Google Scholar: Author Only Title Only Author and Title

Sun S, Yu J-P, Chen F, Zhou T-J, Fang X-H, Li Y-Q, Sui S-F (2008) TINY, a dehydration-responsive element (DRE)-binding protein-like transcription factor connecting the DRE- and ethylene-responsive element-mediated signaling pathways in Arabidopsis. J Biol Chem 283: 6261-6271
Pubmed: Author and Title
CrossRef: Author and Title
Google Scholar: Author Only Title Only Author and Title

Teper-Bamnolker P, Samach A (2005) The flowering integrator FT regulates SEPALLATA3 and FRUITFULL accumulation in Arabidopsis leaves. Plant Cell 17: 2661-2675
Pubmed: Author and Title
CrossRef: Author and Title
Google Scholar: Author Only Title Only Author and Title

Tian C, Zhang X, He J, Yu H, Wang Y, Shi B, Han Y, Wang G, Feng X, Zhang C, Wang J, Qi J, Yu R, Jiao Y (2014) An organ boundary-enriched gene regulatory network uncovers regulatory hierarchies underlying axillary meristem initiation. Mol Sys Biol 10: 755
Pubmed: Author and Title
CrossRef: Author and Title
Google Scholar: Author Only Title Only Author and Title

Ung N, Lal S, Smith HMS (2011a) The role of PENNYWISE and POUND-FOOLISH in the maintenance of the shoot apical meristem in Arabidopsis. Plant Physiol 156: 605-614
Pubmed: Author and Title
CrossRef: Author and Title
Google Scholar: Author Only Title Only Author and Title

Ung N, Smith HMS (2011b) Regulation of shoot meristem integrity during Arabidopsis vegetative development. Plant Signal Behav 6: 1250-1252
Pubmed: Author and Title
CrossRef: Author and Title
Google Scholar: Author Only Title Only Author and Title

Wang J-W, Czech, B, Weigel D (2009) miR156-regulated SPL transcription factors define an endogenous flowering pathway in Arabidopsis thaliana. Cell 138: 738-739
Pubmed: Author and Title
CrossRef: Author and Title
Google Scholar: Author Only Title Only Author and Title

Wang JW (2014) Regulation of flowering time by the miR156-mediated age pathway. J Exp Bot 65: 4723-4730
Pubmed: Author and Title
CrossRef: Author and Title
Google Scholar: Author Only Title Only Author and Title

Wasternak C, Hause B (2013) Jasmonates: biosynthesis, perception, signal transduction and action in plant stress response, growth and development. An update to the 2007 review in Annals of Botany. Ann Bot 111: 1021-1058

Pubmed: Author and Title
CrossRef: Author and Title
Google Scholar: Author Only Title Only Author and Title

Wasternak C, Kombrink E (2010) Jasmonates: structural requirements for lipid-derived signals active in plant stress responses and development. ACS Chem Biol 5: 63-77
Pubmed: Author and Title
CrossRef: Author and Title
Google Scholar: Author Only Title Only Author and Title

Wigge PA, Kim MC, Jaeger KE, Busch W, Schmid M, Lohmann JU, Weigel D (2005) Integration of spatial and temporal information during floral induction in Arabidopsis. Science 309: 1056-1059
Pubmed: Author and Title
CrossRef: Author and Title
Google Scholar: Author Only Title Only Author and Title

Wild M, Achard P (2013) The DELLA protein RGL3 positively contributes to jasmonate/ethylene defense responses. Plant Signal Behav 8: e23891
Pubmed: Author and Title
CrossRef: Author and Title
Google Scholar: Author Only Title Only Author and Title

Wild M, Davière JM, Cheminant S, Regnault T, Baumberger N, Heintz D, Baltz R, Genschik P, Achard P (2012) The Arabidopsis DELLA RGA-LIKE3 is a direct target of MYC2 and modulates jasmonate signaling responses. Plant Cell 24: 3307-3319
Pubmed: Author and Title
CrossRef: Author and Title
Google Scholar: Author Only Title Only Author and Title

Wu G, Park M, Conway S, Wang J-W, Weigel D, Poethig RS (2009) The sequential action of miR156 and miR172 regulates developmental timing in Arabidopsis. Cell 138: 750-759
Pubmed: Author and Title
CrossRef: Author and Title
Google Scholar: Author Only Title Only Author and Title

Wu G, Poethig RS (2006) Temporal regulation of shoot development in Arabidopsis thaliana by miR156 and its target SPL3. Development 133: 3539-3547
Pubmed: Author and Title
CrossRef: Author and Title
Google Scholar: Author Only Title Only Author and Title

Xiang D, Venglat P, Tibiche C, Yang H, Risseeuw E, Cao Y, Babic V, Cloutier M, Keller W, Wang E, Selvaraj G, Datla R (2011) Genome-wide analysis reveals gene expression and metabolic network dynamics during embryo development in Arabidopsis. Plant Physiol 156: 346-356
Pubmed: Author and Title
CrossRef: Author and Title
Google Scholar: Author Only Title Only Author and Title

Xu M, Hu T, McKim SM, Murmu J, Haughn GW, Hepworth SR (2010) Arabidopsis BLADE-ON-PETIOLE1 and 2 promote floral meristem fate and determinacy in a previously undefined pathway targeting APETALA1 and AGAMOUS-LIKE24. Plant J 63: 974-989
Pubmed: Author and Title
CrossRef: Author and Title
Google Scholar: Author Only Title Only Author and Title

Yamaguchi A, Wu MF, Yang L, Wu G, Poethig RS, Wagner D (2009) The microRNA-regulated SBP-Box transcription factor SPL3 is a direct upstream activator of LEAFY, FRUITFULL, and APETALA1. Dev Cell 17: 268-278
Pubmed: Author and Title
CrossRef: Author and Title
Google Scholar: Author Only Title Only Author and Title

Yamaguchi S (2008) Gibberellin metabolism and its regulation. Annu Rev Plant Biol 59: 225-251
Pubmed: Author and Title
CrossRef: Author and Title
Google Scholar: Author Only Title Only Author and Title

Yang D-L, Yao J, Mei C-S, Tong X-H, Zeng L-J, Li Q, Xiao L-T, Sun T, Li J., Deng X-W, Lee CM, Thomashow MF, Yang Y., He Z, He SY (2012) Plant hormone jasmonate prioritizes defense over growth by interfering with gibberellin signaling cascade. Proc Natl Acad Sci USA 109: 1192-2000
Pubmed: Author and Title
CrossRef: Author and Title
Google Scholar: Author Only Title Only Author and Title

Yang L, Xu M, Koo Y, He J, Poethig RS (2013) Sugar promotes vegetative phase change in Arabidopsis thaliana by repressing the expression of MIR156A and MIR156C. eLife 2: e00260
Pubmed: Author and Title
CrossRef: Author and Title
Google Scholar: Author Only Title Only Author and Title

Yang Y, Paquet A, Dudoit S (2009) Package 'marray': exploratory analysis for two-color spotted microarray data. Version 1.42.0.
Pubmed: Author and Title
CrossRef: Author and Title
Google Scholar: Author Only Title Only Author and Title

Yant L, Mathieu J, Dinh TT, Ott F, Lanz C, Wollmann H, Chen X, Schmid M (2010) Orchestration of the floral transition and floral development in Arabidopsis by the bifunctional transcription factor APETALA2. Plant Cell 22: 2156-2170
Pubmed: Author and Title
CrossRef: Author and Title
Google Scholar: Author Only Title Only Author and Title

Yu S, Cao L, Zhou C-M, Zhang T-Q, Lian H, Sun Y, Wu J, Huang J, Wang G, Wang J-W (2013) Sugar is an endogenous cue for juvenile-to-adult phase transition in plants. eLife 2: e00269
Pubmed: Author and Title
CrossRef: Author and Title
Google Scholar: Author Only Title Only Author and Title

Yu S, Galvão VC, Zhang YC, Horrer D, Zhang TQ, Hao YH, Feng YQ, Wang S, Schmid M, Wang JW (2012) Gibberellin regulates the Arabidopsis floral transition through miR156-targeted SQUAMOSA promoter binding-like transcription factors. Plant Cell 24: 3320-3332
Pubmed: Author and Title
CrossRef: Author and Title
Google Scholar: Author Only Title Only Author and Title

Zhang Y, Turner JG (2008) Wound-induced endogenous jasmonates stunt plant growth by inhibiting mitosis. PLoS One 3: e3699
Pubmed: Author and Title
CrossRef: Author and Title
Google Scholar: Author Only Title Only Author and Title

Zhao M, Yang S, Chen C-Y, Li C, Shan W, Lu W, Cui Y, Liu X, K W (2015) Arabidopsis BREVIPEDICELLUS interacts with the SWI2/SNF2 chromatin remodeling ATPase BRAHMA to regulate KNAT2 and KNAT6 expression in control of inflorescence architecture. PLoS Genet 11: e1005125
Pubmed: Author and Title
CrossRef: Author and Title
Google Scholar: Author Only Title Only Author and Title

Zhu Q-H, Helliwell CA (2011) Regulation of flowering time and floral patterning by miR172. J Exp Bot 62: 487-495
Pubmed: Author and Title
CrossRef: Author and Title
Google Scholar: Author Only Title Only Author and Title